DESIGN OF A GEAR REDUCER

Milano, 26 April 2016

Design of the Central Shaft

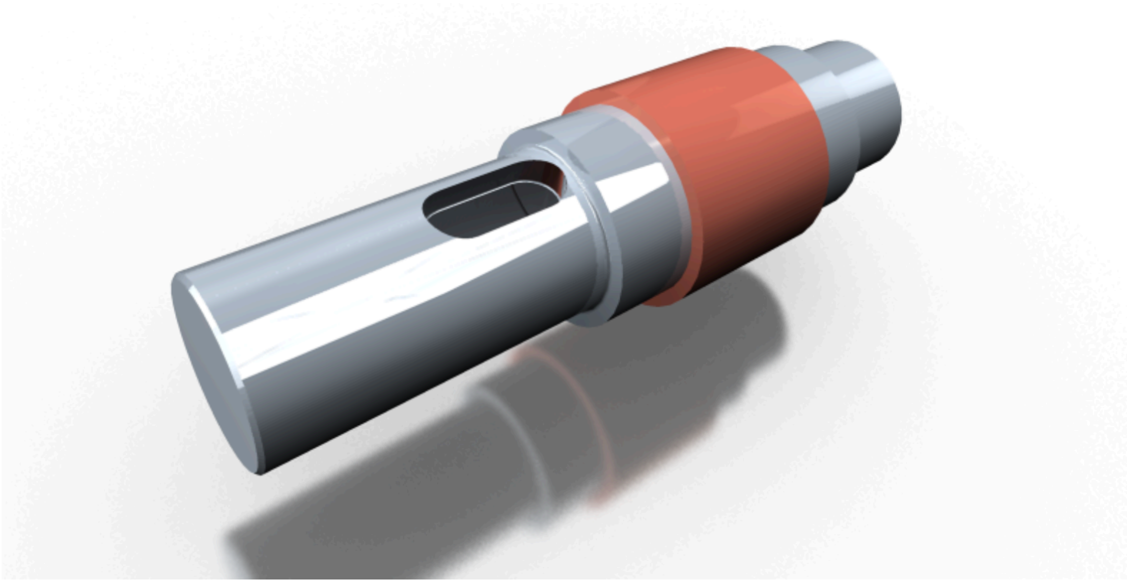

Zhongtian CAI

875870

Milano, 17 Sep 2017

Table of Contents

Introduction

This project is to design the central shaft for a MR 3I 80 UP2A Gear Reducer, with pre-dimensioning and verification under the particular working condition.

An analytical approach will be applied for initial dimensioning of the shafts, taking into consideration of its interactions with other mechanical components in the machine, including bearings, keys and gear teeth. Then a computer modeling process and a finite element method (FEM) will be employed to precisely analyze and verify the overall design.

1. ANALYTICAL DESIGN

In this section, a pre-dimensioning of the central shaft and the verification of bearings, keys and gearing will be presented basing on the calculations and on internal stresses and some specific analytical criterions for failures of specific mechanical components.

1.1. *Design background*

A reduction drive is a mechanical device to shift rotational speed and torque. Typically, reduction drives work through toothed gears and are called ‘gear reducers’. Gear reducers are widely used in mechanical industry, because generally the motors operate only within a limited range of rotating speed, and the gear reducers easily shift the output speed and torque to a desired value. For example, the gearbox of the transmission in the vehicles is a system with advanced application of gear reducers.

1.1.1 Reducer Model

The interested gear reducer, model MR 3I 80 UP2A, is characterized by three parallel shafts and thus three gearing pairs, a final wheelbase of 80mm. In the nominal condition it should be universally mounted, and the coupled electric motor should be a three-phase asynchronous motor with cage rotor with a maximum two minutes of one or more overloads each hour, and a maximum input torque of 1.6 times of nominal torque.

1.1.2 Component to design

This project is focused on the main central shaft, which is in between the other two shafts, transmitting the torque from one to another. The power flows into the central shaft on the right through a wheel gear connected with a key, and flows out on the left with gear tooth geometry of on the shaft itself. The shaft is supported on each end by one rolling gearing, which can be considered as constraints of cart on one side and hinge on the other side. The design of the shaft has to meet the general failure criterions, which are mostly related with the material properties, to ensure a stable performance and security under an expected working condition.

1.2. *Data and the design specifications*

The input power $P_{in} = 0.5\text{kW} + 0.2\text{kW}\times 0 = 0.5\text{kW}$
The output rotating speed $n_u = 25 + 0.2\times 12 = 27.4\text{rpm}$
The total transmission ratio $u = 41.7$
The (gear 1-2) transmission ratio $u_{1-2} = 2$
The (gear 3-4) transmission ratio $u_{3-4} = 5$
The pressure angle $\alpha_n = 20°$
The efficiency of the gear motor is 1

1.3. *Design and Verification for Gears*

In this section, a dimensioning and verification of the gear pair No.3&4 and No.5&6 will be carried out, with the given overall design of the gearbox and some of the unknown parameters calculated in the following sections.
The given working conditions are:

A. Engine and machine operated operating characteristics: a few overloads;
   Number of design cycles for the smallest wheel: 108
B. Lubricant: oil ISO VG 220
C. Operating temperature: 60 °C
D. Superficial hardness of drive and conducted gears: HB 650

1.3.1 Gear Pair No.3&4

A. Dimensioning

As is instructed, the model MR 3I 80 UP2A has fixed distance among each shaft. So according to the original model design, we have

$$\begin{cases} a_{3-4} = 62.5 \text{ mm} \\ u_{3-4} = 5 \end{cases} \Longrightarrow \begin{cases} d_{p3,theory} = \dfrac{2a_{3-4}}{u_{3-4}+1} = 20.83 \text{ mm} \\ d_{p4,theory} = u_{3-4}\cdot d_{p3,theory} = 104.17 \text{ mm} \end{cases}$$

With the superficial synthetic factor $K^* = K$ and tooth-foot factor $U_L{}^*$ chosen from the standards and tables given in 《Es10 - Dimensionamento Di Ruote Dentate》 (Page 5&6), we can write

$$\begin{cases} b_{3-4} = \dfrac{1}{K^*}\cdot\dfrac{2C_3}{d_{p3,theory}}\cdot\dfrac{u_{3-4}+1}{u_{3-4}} \\ C_3 = \dfrac{P}{\omega_1} \end{cases} \Longrightarrow \quad b_{3-4} = 6.26 \text{ mm}$$

$$\begin{cases} m_{n,3} = m_{n,4} = \dfrac{F_{t,3-4}}{b\cdot U_L{}^*} \\ F_{t,3-4} = \dfrac{2C_3}{d_{p3,theory}} \end{cases} \Longrightarrow \quad m_{n,3} = m_{n,4} = 1.21$$

So according to the experience, it is decided that $m_{n,3-4} = 1.25$. Thus,

$$m_{t,3} = m_{t,4} = \frac{m_{n,3}}{\cos\beta_{3-4}} = \frac{1.25}{\cos 16°16'} = 1.3021$$

$$\Longrightarrow \begin{cases} z_3 = \dfrac{d_{p3,theory}}{m_{t,3-4}} \approx 16 \\ z_4 = u_{3-4} \cdot z_3 = 80 \end{cases}$$

Since

$$z_{min} = \frac{2}{\sin^2 \alpha} \approx 17 \Longrightarrow z_3 < z_{min}$$

we will have phenomenon called ‘undercutting’ during producing the gear No.3. As a result, we apply profile displacement to the gear pair and try to find the displacement coefficient x:

$$z'_{min} = \frac{2(1-x)}{\sin^2 \alpha} < z_3 = 16 \Longrightarrow x > 0.064$$

So we make $x = 0.1$. And, with the calculated teeth number,

$$\begin{cases} d_{p3} = d_{p3,real} = z_3 \cdot m_{t,3} = 20.83 \text{ mm} \\ d_{p4} = d_{p4,real} = z_4 \cdot m_{t,4} = 104.17 \text{ mm} \end{cases} \Longrightarrow u_{3-4,real} = \frac{z_4}{z_3} = 5.001$$

which means that the result in fact perfectly meets the need, so the dimensioning is reasonable.

B. Verification of Pitting

Referring to the Standard UNI 8862:1987, to verify the pitting, the following formula should be guaranteed:

$$\sigma_H = \mathrm{Z}_H \mathrm{Z}_E \mathrm{Z}_\varepsilon \mathrm{Z}_\beta \sqrt{\frac{F_t}{b \cdot d_p} \cdot \frac{u+1}{u}} \sqrt{K_A K_V K_{H\alpha} K_{H\beta}} \leq \sigma_{HP} = \frac{\sigma_{H,lim} Z_N}{S_{H,lim}} \mathrm{Z}_L \mathrm{Z}_R \mathrm{Z}_V \mathrm{Z}_W \mathrm{Z}_X$$

From the given tables and texts of UNI 8862:1987, we have

$$K_A = 1.5$$

$$\frac{Vz}{100} = 0.53 \Longrightarrow K_V \approx 1$$

$$K_{H\alpha} = 1$$

$$K_{H\beta} = 1.4$$

$$\mathrm{Z}_E = \sqrt{\frac{1}{\pi \cdot \left(\dfrac{1-{v_1}^2}{E_1} + \dfrac{1-{v_2}^2}{E_2}\right)}} \approx 190$$

$$\begin{cases} \mathrm{Z}_H = \sqrt{\dfrac{2\cos\beta_b}{\cos\alpha_t \sin\alpha_t}} \Longrightarrow \mathrm{Z}_H = 2.4 \\ \sin\beta_b = \sin\beta \cdot \cos\alpha_n \end{cases}$$

$$\mathrm{Z}_\varepsilon = \sqrt{\frac{4-\varepsilon_\alpha}{2}\left(1-\varepsilon_\beta\right) + \frac{\varepsilon_\beta}{\varepsilon_\alpha}} = 0.658$$

$$\mathrm{Z}_\beta = \sqrt{\cos\beta} = 0.979$$

According to the superficial hardness and its conversion into HRC, we get

$$\sigma_{H,lim} = 1650 \text{ MPa}$$

$$S_{H,lim} = 1.5$$

$$Z_N = 1.6$$

$$R_a = 0.25\ \mu\text{m} \Longrightarrow \mathrm{Z}_R = 1.125$$

$$\mathrm{Z}_V = 0.95$$

$$\mathrm{Z}_L = 0.98$$

$$\mathrm{Z}_W = 1$$

$$Z_X = 1$$

Thus we have

$$\begin{cases} \sigma_H = 2.4\times190\times0.658\times0.979\sqrt{\dfrac{760}{6.26\times20.83}\cdot\dfrac{5+1}{5}}\sqrt{1.5\times1\times1\times1.4} \approx 1126 \text{ MPa} \\ \sigma_{HP} = \dfrac{1650 \text{ MPa} \times1.6}{1.5}\times0.98\times1.125\times0.95\times1\times1 = 1843.38 \text{ MPa} \end{cases}$$

$$\Longrightarrow \sigma_H < \sigma_{HP}$$

So the pitting of the Gear Pair No. 3&4 is verified.

C. Verification of Flexion

Similarly, according to the Standard UNI 8862:1987, it is needed to verify that

$$\sigma_F = Y_{Fa}Y_{Sa}Y_\varepsilon Y_\beta \cdot \frac{F_t}{b\cdot m_n}\cdot K_A K_V K_{F\alpha}K_{F\beta} \le \sigma_{FP} = \frac{\sigma_{F,lim}Y_{ST}Y_{NT}}{S_{F,lim}}Y_{\delta relT}Y_{RrelT}Y_X$$

We have

$$K_A = 1.5$$
$$K_V \approx 1$$
$$K_{F\alpha} = K_{H\alpha} = 1$$

$$\begin{cases} b_{3-4} = 6.26 \text{ mm} \\ h = 2.25m_{n,3} = 2.7225\text{mm} \end{cases} \Longrightarrow n = \frac{\left(\frac{b}{h}\right)^2}{1+\frac{b}{h}+\left(\frac{b}{h}\right)^2} = 0.616 \Longrightarrow K_{F\beta} = \left(K_{H\beta}\right)^n = 1.23$$

According to the given diagrams and formulas, we can get

$$Y_{Fa} = 2.25$$
$$Y_{Sa} = 1.9$$
$$Y_\varepsilon = 0.25 + \frac{0.75}{\varepsilon_\alpha} = 0.66$$
$$Y_\beta = 0.94$$
$$Y_{ST} = 2$$
$$Y_{NT} = 1.1$$
$$Y_{\delta relT} = 0.98$$
$$Y_{RrelT} = 1$$
$$Y_X = 1$$
$$\sigma_{F,lim} = 525 \text{ MPa}$$
$$S_{F,lim} = 1.2$$

Thus we have,

$$\begin{cases} \sigma_F = 2.25\times1.9\times0.66\times0.94\times\dfrac{760}{0.00626\times1.21}\times1.5\times1\times1\times1.23 \approx 491 \text{ MPa} \\ \sigma_{FP} = \dfrac{525 \text{ MPa}\times2\times1.1}{1.2}\times0.98\times1\times1 \approx 943 \text{ MPa} \end{cases}$$

$$\Longrightarrow \sigma_F < \sigma_{FP}$$

So the flexion of the Gear Pair No. 3&4 is verified.

1.3.2 Gear Pair No.5&6

A. Dimensioning

Similar as previous calculation on gear pair No.3&4, we can write:

$$\begin{cases} a_{5-6} = 80 \text{ mm} \\ u_{5-6} = 4.17 \end{cases} \Rightarrow \begin{cases} d_{p5,theory} = \dfrac{2a_{5-6}}{u_{5-6}+1} = 31.0 \text{ mm} \\ d_{p6,theory} = u_{5-6} \cdot d_{p5,theory} = 129.0\text{mm} \end{cases}$$

$$\begin{cases} b_{5-6} = \dfrac{1}{K^*} \cdot \dfrac{2C_5}{d_{p5,theory}} \cdot \dfrac{u_{5-6}+1}{u_{5-6}} \\ C_5 = \dfrac{P}{\omega_2} \end{cases} \Rightarrow \quad b_{5-6} = 14.60 \text{ mm}$$

$$\begin{cases} m_{n,5} = m_{n,6} = \dfrac{F_{t,5-6}}{b \cdot {U_L}^*} \\ F_{t,5-6} = \dfrac{2C_5}{d_{p5,theory}} \end{cases} \Rightarrow \quad m_{n,5} = m_{n,6} = 1.751$$

So according to the experience, it is decided that $m_{n,5-6} = 2$. Thus,

$$m_{t,5} = m_{t,6} = \frac{m_{n,5}}{\cos \beta_{5-6}} = \frac{2}{\cos 14°22'} = 2.0646$$

$$\Rightarrow \begin{cases} z_5 = \dfrac{d_{p5,theory}}{m_{t,5-6}} \approx 15 \\ z_6 = u_{5-6} \cdot z_5 \approx 62 \end{cases} \Rightarrow \quad z_5 < z_{min} = 17$$

Thus ‘undercutting’ is present.

$$z'_{min} = \frac{2(1-x)}{\sin^2 \alpha} < z_3 = 15 \Rightarrow x > 0.123$$

Make $x = 0.15$.

$$\Rightarrow \begin{cases} d_{p5} = d_{p5,real} = z_5 \cdot m_{t,5} = 30.97 \text{ mm} \\ d_{p6} = d_{p6,real} = z_6 \cdot m_{t,6} = 128.03 \text{ mm} \end{cases} \Rightarrow u_{5-6,real} = \frac{z_6}{z_5} = 4.133$$

The difference between the real transmission ratio and the required one is about 0.89%, which is on the whole an acceptable error, which makes the dimensioning reasonable enough.

B. Verification of Pitting

Similar with the procedure of the verification of Gear 4, we can have, again,

$$\sigma_H = Z_H Z_E Z_\varepsilon Z_\beta \sqrt{\frac{F_t}{b \cdot d_p} \cdot \frac{u+1}{u}} \sqrt{K_A K_V K_{H\alpha} K_{H\beta}} \le \sigma_{HP} = \frac{\sigma_{H,lim} Z_N}{S_{H,lim}} Z_L Z_R Z_V Z_W Z_X$$

We have

$$K_A = 1.5$$

$$\frac{Vz}{100} = 0.59 \Rightarrow K_V \approx 1$$

$$K_{H\alpha} = 1$$

$$K_{H\beta} = 1.4$$

$$Z_E = \sqrt{\frac{1}{\pi \cdot \left(\dfrac{1-{v_1}^2}{E_1} + \dfrac{1-{v_2}^2}{E_2} \right)}} \approx 192$$

$$\begin{cases} Z_H = \sqrt{\dfrac{2\cos\beta_b}{\cos\alpha_t \sin\alpha_t}} \Rightarrow Z_H = 2.4 \\ \sin\beta_b = \sin\beta \cdot \cos\alpha_n \end{cases}$$

$$Z_\varepsilon = \sqrt{\frac{4-\varepsilon_\alpha}{2}\left(1-\varepsilon_\beta\right) + \frac{\varepsilon_\beta}{\varepsilon_\alpha}} = 0.66$$

$$Z_\beta = \sqrt{\cos\beta} = 0.979$$

According to the superficial hardness and its conversion into HRC, we get

$$\sigma_{H,lim} = 1650 \text{ MPa}$$
$$S_{H,lim} = 1.5$$
$$Z_N = 1.6$$
$$R_a = 0.25\ \mu\text{m} \Rightarrow Z_R = 1.125$$
$$Z_V = 0.95$$
$$Z_L = 0.98$$
$$Z_W = 1$$
$$Z_X = 1$$

Thus we have

$$\begin{cases} \sigma_H = 2.4 \times 192 \times 0.66 \times 0.979 \sqrt{\dfrac{2557}{14.6 \times 30.97} \cdot \dfrac{4.133+1}{4.133}} \sqrt{1.5 \times 1 \times 1 \times 1.4} \approx 1144 \text{ MPa} \\ \sigma_{HP} = \dfrac{1650 \text{ MPa} \times 1.6}{1.5} \times 0.98 \times 1.125 \times 0.95 \times 1 \times 1 = 1843.38 \text{ MPa} \end{cases}$$

$$\Rightarrow \sigma_H < \sigma_{HP}$$

So the pitting of the Gear Pair No. 5&6 is verified.

C. Verification of Flexion

Similarly, it is needed to verify that

$$\sigma_F = Y_{Fa} Y_{Sa} Y_\varepsilon Y_\beta \cdot \frac{F_t}{b \cdot m_n} \cdot K_A K_V K_{F\alpha} K_{F\beta} \le \sigma_{FP} = \frac{\sigma_{F,lim} Y_{ST} Y_{NT}}{S_{F,lim}} Y_{\delta relT} Y_{RrelT} Y_X$$

We have

$$K_A = 1.5$$
$$K_V \approx 1$$
$$K_{F\alpha} = K_{H\alpha} = 1$$

$$\begin{cases} b_{3-4} = 14.60 \text{ mm} \\ h = 2.25 m_{n,3} = 3.94 \text{ mm} \end{cases} \Rightarrow n = \frac{\left(\frac{b}{h}\right)^2}{1 + \frac{b}{h} + \left(\frac{b}{h}\right)^2} = 0.7448 \Rightarrow K_{F\beta} = \left(K_{H\beta}\right)^n = 1.285$$

According to the given diagrams and formulas, we can get

$$Y_{Fa} = 2.75$$
$$Y_{Sa} = 1.47$$
$$Y_\varepsilon = 0.25 + \frac{0.75}{\varepsilon_\alpha} = 0.50$$
$$Y_\beta = 0.94$$
$$Y_{ST} = 2$$
$$Y_{NT} = 1$$

$$Y_{\delta relT} = 0.98$$
$$Y_{RrelT} = 1$$
$$Y_X = 1$$
$$\sigma_{F,lim} = 525\text{ MPa}$$
$$S_{F,lim} = 1.2$$

Thus we have,

$$\begin{cases} \sigma_F = 2.75\times1.47\times0.50\times0.94\times\dfrac{2557}{0.0146\times0.001751}\times1.5\times1\times1\times1.285 \approx 367\text{ MPa} \\ \sigma_{FP} = \dfrac{525\text{ MPa}\times2\times1.1}{1.2}\times0.98\times1\times1 \approx 943\text{ MPa} \end{cases}$$
$$\Longrightarrow \sigma_F < \sigma_{FP}$$

So the flexion of the Gear Pair No. 5&6 is verified.

1.4. *Calculation of the Loads*

1.4.1 Description of the system: power flow

The power flow of the system is clearly illustrated in Fig 1. The input power is transmitted into shaft 1, then shaft 2 (the central one, the interested one in this project) through gear pair No. 3&4. At last the power is transmitted through gear pair No. 5&6 into the output shaft.

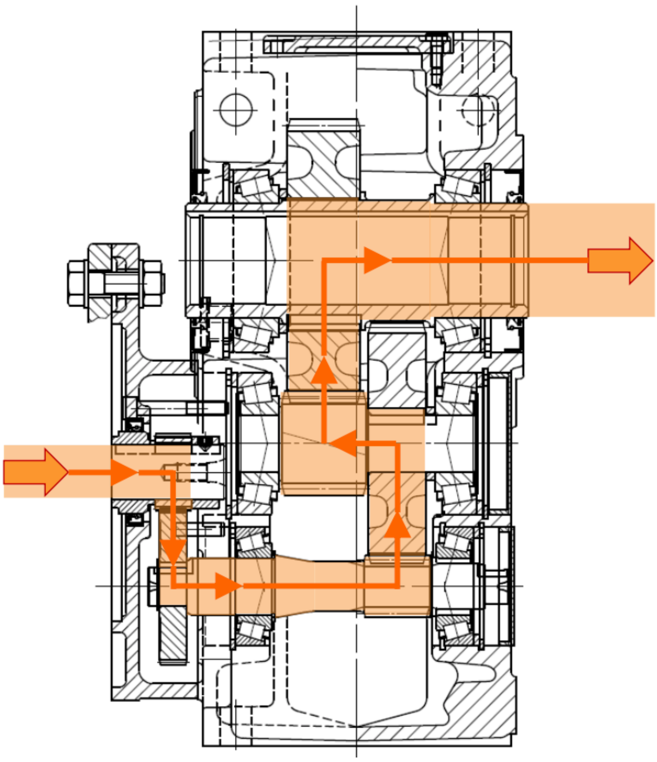

Fig 1: ILLUSTRATION OF THE POWER FLOW

1.4.2 Calculations of the forces generated within gears

$$P = \omega \cdot C \Longrightarrow C_{out} = \frac{P_{out}}{\omega_{out}} = \frac{P_{out}}{\frac{2\pi n_{out}}{60}} = 186.51\text{ N}\cdot\text{m}$$

$$n_{in} = u \cdot n_{out} = 47.1 \times 25.6 = 1205.76 \text{ rpm}$$

$$P_{in} = \frac{P_{out}}{\eta} = P_{out} = P \Longrightarrow C_{in} = \frac{P_{in}}{\omega_{in}} = \frac{P_{in}}{\frac{2\pi n_{in}}{60}} = 3.96 \text{ N} \cdot \text{m}$$

$$\omega_1 = \frac{2\pi \left(\frac{n_{in}}{u_{1-2}}\right)}{60} = 63.13 \text{ rad/s}$$

Thus for the central shaft, we have the rotating speed and the torque:

$$\omega_2 = \frac{2\pi \left(\frac{n_{in}}{u_{1-2} \cdot u_{3-4}}\right)}{60} = 12.63 \text{ rad/s}$$

$$C = C_2 = M_t = \frac{P}{\omega_2} = 39.59 \text{ N} \cdot \text{m}$$

As was calculated previously, we have:

$$\begin{cases} d_{p4} = m_{t4} \cdot z_4 = 104.17 \text{ mm} \\ d_{p5} = m_{t5} \cdot z_5 = 30.97 \text{ mm} \end{cases}$$

Thus, for Gear 4:

$$\begin{cases} F_{t4} = \dfrac{2C}{d_{p4}} = 760.14 \text{ N} \\ F_{a4} = F_{t4} \cdot \tan\beta_4 = 221.80 \text{ N} \\ F_{r4} = F_{t4} \cdot \dfrac{\tan\alpha_n}{\cos\beta_4} = 288.21 \text{ N} \end{cases}$$

and for Gear 5:

$$\begin{cases} F_{t5} = \dfrac{2C}{d_{p5}} = 2556.67 \text{ N} \\ F_{a5} = F_{t5} \cdot \tan\beta_5 = 654.86 \text{ N} \\ F_{r5} = F_{t5} \cdot \dfrac{\tan\alpha_n}{\cos\beta_5} = 960.59 \text{ N} \end{cases}$$

1.4.3 Calculations of the reaction forces on the supports

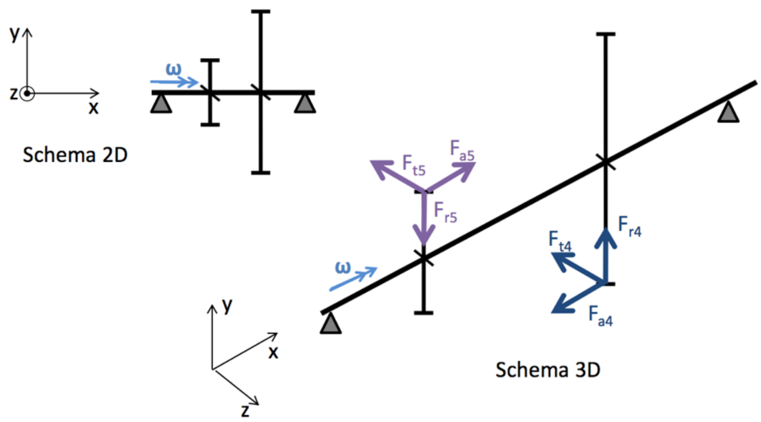

Fig 2: ILLUSTRATION OF ALL THE FORCES PARTICIPATING

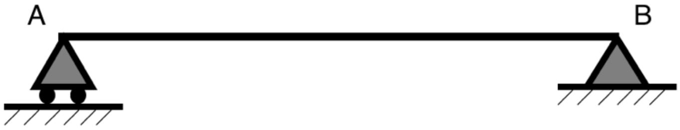

Fig 3: ILLUSTRATION OF THE CONSTRAINTS

Suppose the constraint types to be cart on the left and hinge on the right, as is illustrated in Fig 3.

The axial constraint forces are therefore:

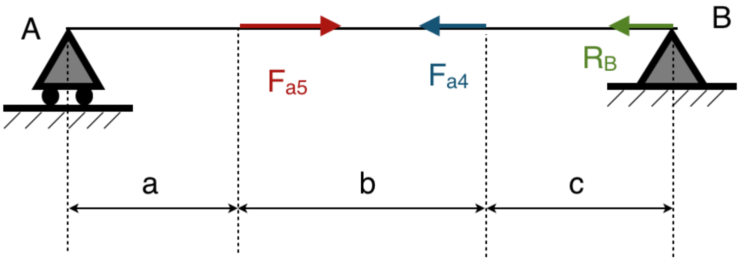

Fig 4: AXIAL CONSTRAINT FORCES

$$F_{a5} - F_{a4} - R_B = 0$$
$$\Longrightarrow R_B = 433.06 \text{ N}$$

On the radial-axial plane (XY plane),

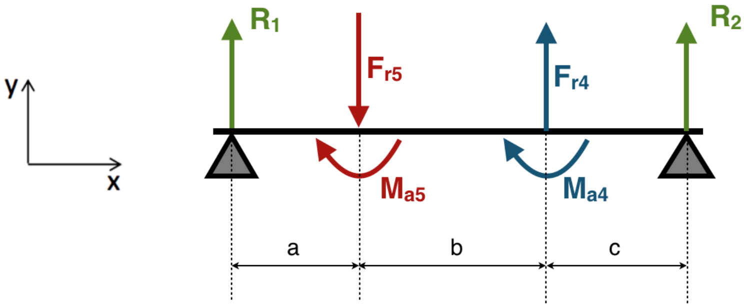

Fig 5: FORCES ON XY PLANE

$$\begin{cases} R_1 + R_2 + F_{r4} - F_{r5} = 0 \\ F_{r5} \cdot a + M_{a5} - F_{r4} \cdot (a+b) + M_{a4} - R_2(a+b+c) = 0 \\ M_{a5} = F_{a5} \cdot \dfrac{d_{p5}}{2};\ M_{a4} = F_{a4} \cdot \dfrac{d_{p4}}{2} \end{cases}$$

And from the given technical drawing, it is found that

$$a = 37.5\text{mm}; b = 34\text{mm}; c = 32.5\text{mm}$$

Thus we have

$$\begin{cases} R_1 = 315.58 \text{ N} \\ R_2 = 356.80 \text{ N} \end{cases}$$

Similarly, on the XZ plane,

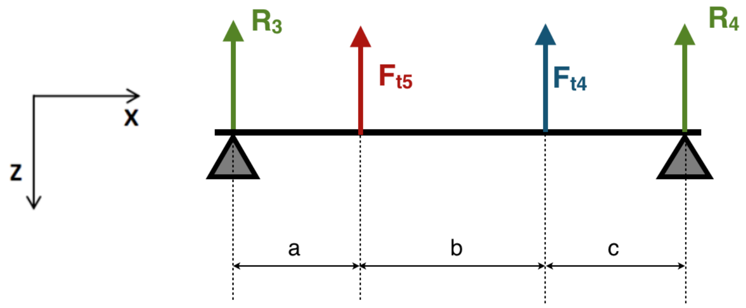

Fig 6: FORCES ON XZ PLANE

$$\begin{cases} R_3 + R_4 + F_{t4} + F_{t5} = 0 \\ F_{t5} \cdot a + F_{t4} \cdot (a + b) + R_4 \cdot (a + b + c) = 0 \end{cases}$$

thus,

$$\begin{cases} R_3 = -1872.30 \text{ N} \\ R_4 = -1444.50 \text{ N} \end{cases}$$

1.4.4 Diagram of the internal forces in the shaft

Axial forces:

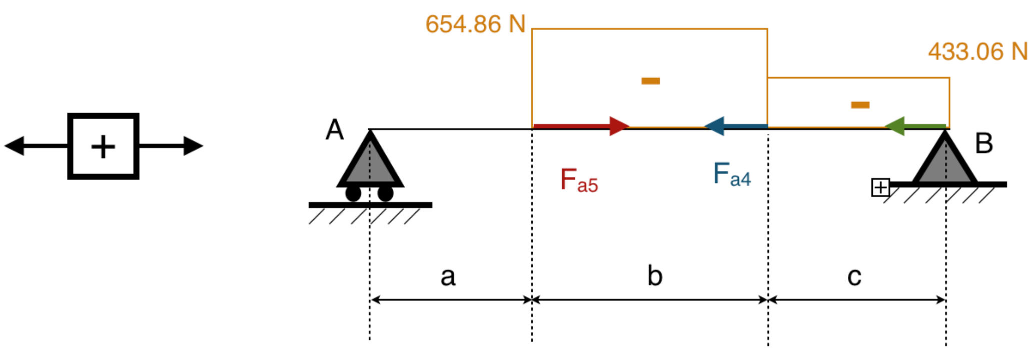

Fig 7: INTERNAL AXIAL FORCES

Torque:

$$M_{t4} = M_{t5} = M_t = C = 39.59 \text{ N} \cdot \text{m}$$

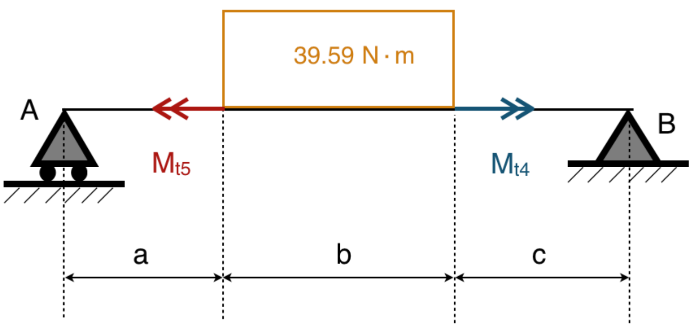

Fig 8: INTERNAL TORQUE

Shear forces and bending moments on the radial-axial plane (XY plane):

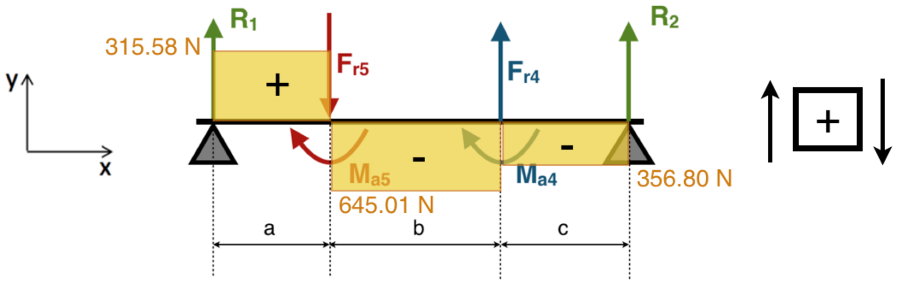

Fig 9: INTERNAL SHEAR FORCES ON XY PLANE

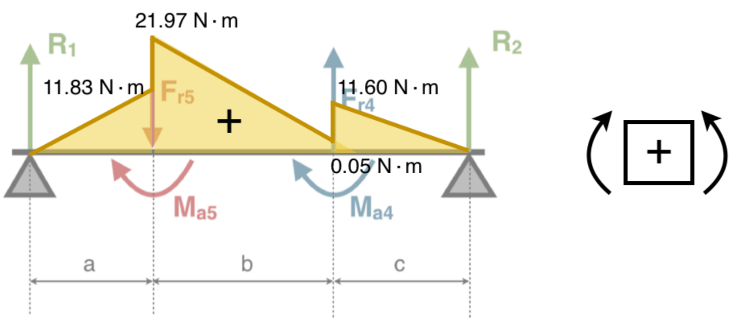

Fig 10: INTERNAL BENDING MOMENTS ON XY PLANE

Shear forces and bending moments on the tangential-axial plane (XZ plane):

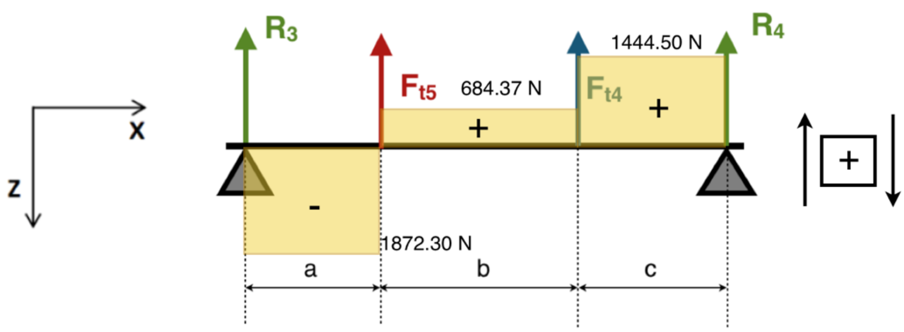

Fig 11: INTERNAL SHEAR FORCES ON XZ PLANE

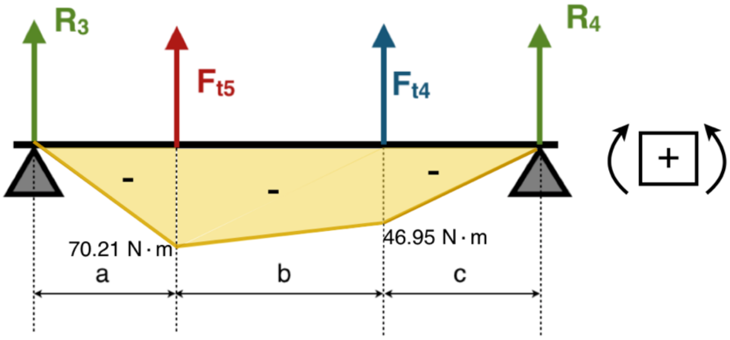

Fig 12: INTERNAL BENDING MOMENTS ON XZ PLANE

1.5. *Dimensioning of the Central Shaft and Verifications*

1.5.1 Dimensioning

$$\sigma_{eq} = \frac{32M_{f,eq}}{\pi d^3} \le \sigma_{amm} \Rightarrow d \ge 2.17\sqrt[3]{\frac{M_{f,eq}}{\sigma_{amm}}}$$

$$\sigma_{amm} = \frac{R_m}{6} = 171.67 \text{ MPa}$$

$$M_{f,eq} = \sqrt{{M_{f,max}}^2 + (\alpha \cdot M_{t,max})^2}$$

$$\begin{cases} M_{f,max} = \sqrt{{M_{f,max,XY}}^2 + {M_{f,max,XZ}}^2} = 73.57 \text{ N}\cdot\text{m} \\ M_{t,max} = 39.59 \text{ N}\cdot\text{m} \end{cases}$$

As the torque is considered quasi-constant, we have:

$$\alpha^2 = 0.25$$

thus,

$$M_{f,eq} = 76.20 \text{ N}\cdot\text{m}$$

$$\Rightarrow d \ge 2.17\sqrt[3]{\frac{M_{f,eq}}{\sigma_{amm}}} \approx 16.55 \text{ mm}$$

To leave the machine with an adequate safety margin, make the $d = 22$ mm.

1.5.2 Static Verification

According to the given property of the asynchronous three-phase electric motor,

$$C_{start-up} = C_{max} = 1.6C_{nom}$$

and the static varication should be carried out under the critical condition, with the torque being maximum, and the test position being the exact point with both maximum axial and shear stress at the same time. Supposing an adequate safety factor $\eta = 1.5$, we have:

$$\sigma_{start-up} \approx 1.6\sigma_{max,nom} = 1.6\frac{32M_{f,max}}{\pi d^3} = 112.60 \text{ MPa}$$

$$\tau_{start-up} = 1.6\tau_{max,nom} = 1.6\frac{16M_t}{\pi d^3} = 30.30 \text{ MPa}$$

$$\Rightarrow \sigma_{vM} = \sqrt{\sigma_{start-up}{}^2 + 3 \cdot \tau_{start-up}{}^2} = 116.61 \text{ MPa}$$

$$\sigma_{amm} = \frac{R_{sn}}{\eta} = \frac{735}{1.5} = 490 \text{ MPa}$$

$$\Rightarrow \sigma_{vM} < \sigma_{amm}$$

So we have the shaft verified in the static condition.

1.5.3 Fatigue Verification

According to the parameters of the gear teeth and the pre-dimensioning in chapter 1.4.2, it can be deduced:

$$\begin{cases} D/d = 27/22 = 1.23 \\ r/d = 0.6/20 = 0.03 \end{cases}$$

thus according to the Fig 13 (left part), we have:

$$K_{t,f} \approx 2.20$$

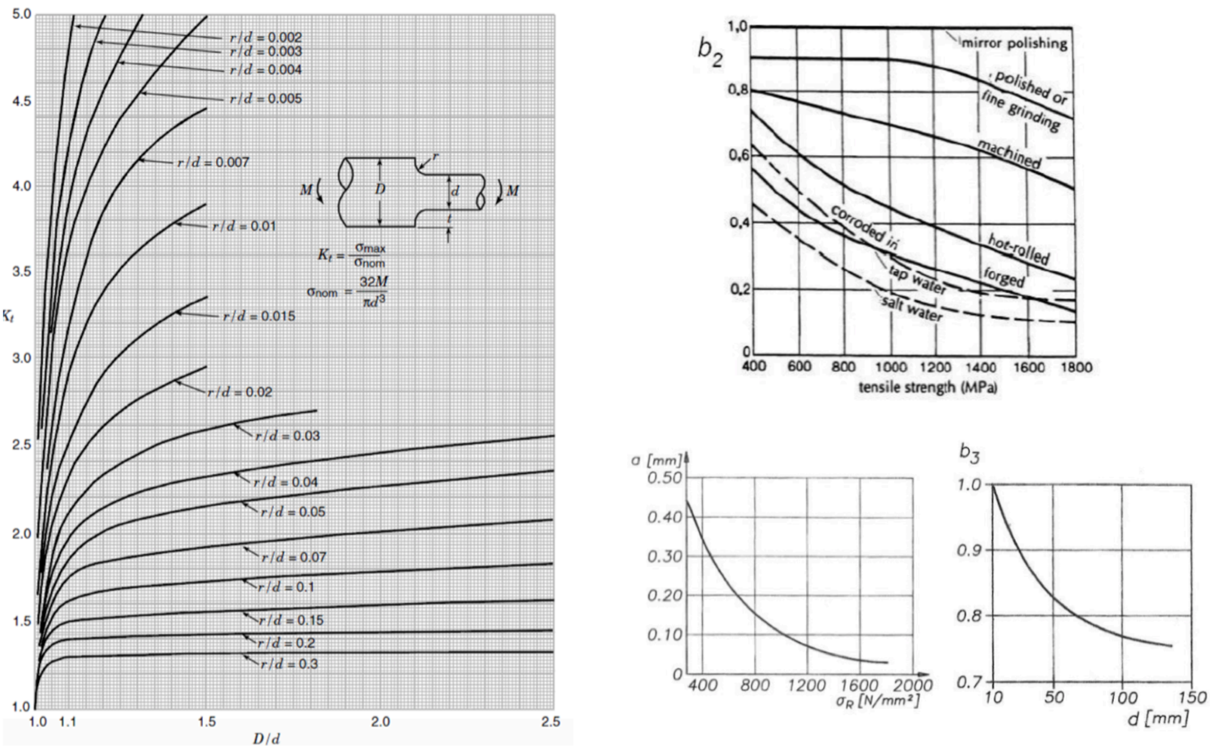

Fig 13: TABLES COEFFICIENT USED IN FATIGUE ANALYSIS

According to Peterson's relation, we have the notch sensibility

$$q = \frac{1}{1 + a/r}$$

and from the Fig 13 (right part) it is found that

$$a \approx 0.1$$

$$\Rightarrow q = 0.86$$

Thus,

$$K_{f,f} = 1 + q(K_{t,f} - 1) = 2.032$$

We assume the bending moment to be fatigue and the torque to be static, so

$$\begin{cases} \sigma_{lim} = \dfrac{b_2 b_3}{K_{f,f}} \sigma_F = \dfrac{b_2 b_3}{K_{f,f}} \cdot 0.5 R_m \\ \tau_{lim} = 0.58 R_{sn} \end{cases}$$

and also, by taking into account only the alternative component of tensile stress, which is the bending moment, and supposing the alternative component of shear stress to be its medium, we get:

$$\begin{cases} \sigma_a = \dfrac{32 M_{f,max}}{\pi d^3} = 70.38 \text{ MPa} \\ \tau_a = \tau_m = \dfrac{16 M_t}{\pi d^3} = 18.94 \text{ MPa} \end{cases}$$

According to Fig 13 (right part) we can find

$$b_2 = 0.9;\ b_3 = 0.7$$

Thus,

$$\begin{cases} \sigma_{lim} = \dfrac{0.9 \times 0.7}{2.07} \times 0.5 \times 1030 = 156.73 \text{ MPa} \\ \tau_{lim} = 0.58 \times 735 = 426.30 \text{ MPa} \end{cases}$$

$$\Rightarrow H = \frac{\sigma_{lim}}{\tau_{lim}} = 0.37$$

Using the Gough-Pollard criterion, we can write

$$\sigma^*{}_{GP} = \sqrt{\sigma_a{}^2 + H^2 \tau_a{}^2} = 70.72 \text{ MPa}$$

$$\sigma_{amm} = \frac{\sigma_{lim}}{\eta} = \frac{215.85}{1.5} = 143.9 \text{ MPa}$$

$$\Rightarrow \sigma^*{}_{GP} < \sigma_{amm}$$

As a result, the fatigue condition is also verified.

1.5.4 Verification of deformation: deflection and rotation

The deformation in forms of deflection and rotation can be calculated from PLV and the superposition method.

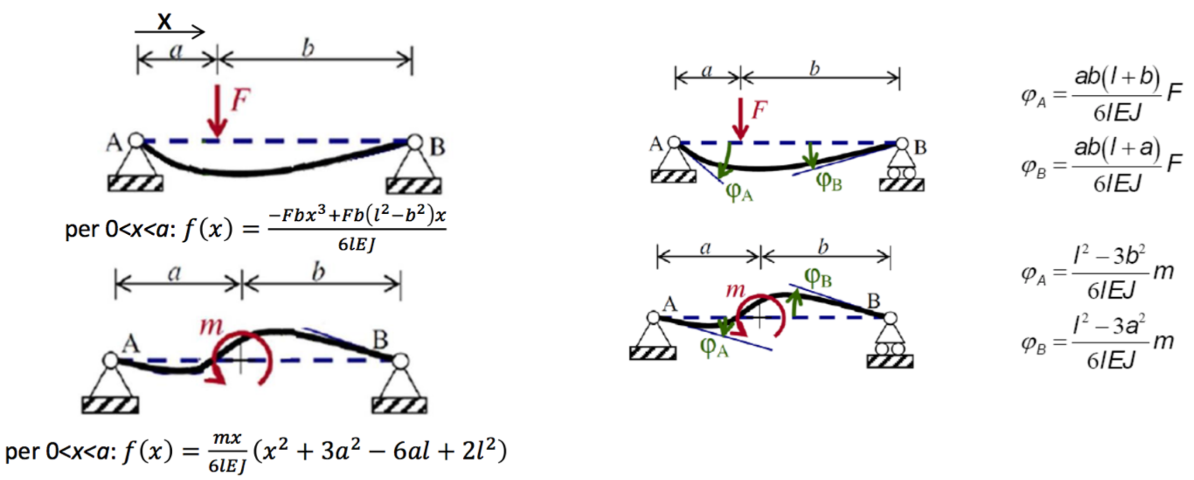

Fig 14: TABLES OF TYPICAL DEFORMATIONS BY PLV

For 16MnCr5, elastic modulus $E = 210$ GPa, the section inertia $J = \frac{\pi d^4}{64} = 1.15\times10^{-8}\ \mathrm{m}^4$.
In XY plane:

$$\begin{cases} f_4{}^{(1)} = f_{F_{r4}\to 4} = 2.1\times10^{-3}\ \mathrm{mm} \\ f_5{}^{(1)} = f_{F_{r4}\to 5} = 1.9\times10^{-3}\ \mathrm{mm} \\ \varphi_A{}^{(1)} = \varphi_{F_{r4}\to A} = 6.07\times10^{-5}\ \mathrm{rad} \\ \varphi_B{}^{(1)} = \varphi_{F_{r4}\to B} = 7.80\times10^{-5}\ \mathrm{rad} \end{cases} \qquad \begin{cases} f_4{}^{(2)} = f_{F_{r5}\to 4} = -6.5\times10^{-3}\ \mathrm{mm} \\ f_5{}^{(2)} = f_{F_{r5}\to 5} = -7.9\times10^{-3}\ \mathrm{mm} \\ \varphi_A{}^{(2)} = \varphi_{F_{r5}\to A} = -2.71\times10^{-4}\ \mathrm{rad} \\ \varphi_B{}^{(2)} = \varphi_{F_{r5}\to B} = -2.25\times10^{-4}\ \mathrm{rad} \end{cases}$$

$$\begin{cases} f_4{}^{(3)} = f_{M_{a4}\to 4} = 1.4\times10^{-3}\ \mathrm{mm} \\ f_5{}^{(3)} = f_{M_{a4}\to 5} = 1.8\times10^{-3}\ \mathrm{mm} \\ \varphi_A{}^{(3)} = \varphi_{M_{a4}\to A} = 5.86\times10^{-5}\ \mathrm{rad} \\ \varphi_B{}^{(3)} = \varphi_{M_{a4}\to B} = -3.47\times10^{-5}\ \mathrm{rad} \end{cases} \qquad \begin{cases} f_4{}^{(4)} = f_{M_{a5}\to 4} = -1.2\times10^{-3}\ \mathrm{mm} \\ f_5{}^{(4)} = f_{M_{a5}\to 5} = -0.97\times10^{-3}\ \mathrm{mm} \\ \varphi_A{}^{(4)} = \varphi_{M_{a5}\to A} = 1.65\times10^{-5}\ \mathrm{rad} \\ \varphi_B{}^{(4)} = \varphi_{M_{a5}\to B} = -4.44\times10^{-5}\ \mathrm{rad} \end{cases}$$

$$\Rightarrow \begin{cases} f_{4,XY} = f_4{}^{(1)} + f_4{}^{(2)} + f_4{}^{(3)} + f_4{}^{(4)} = -4.2\times10^{-3}\ \mathrm{mm} \\ f_{5,XY} = f_5{}^{(1)} + f_5{}^{(2)} + f_5{}^{(3)} + f_5{}^{(4)} = -5.17\times10^{-3}\ \mathrm{mm} \\ \varphi_{A,XY} = \varphi_A{}^{(1)} + \varphi_A{}^{(2)} + \varphi_A{}^{(3)} + \varphi_A{}^{(4)} = -1.35\times10^{-4}\ \mathrm{rad} \\ \varphi_{B,XY} = \varphi_B{}^{(1)} + \varphi_B{}^{(2)} + \varphi_B{}^{(3)} + \varphi_B{}^{(4)} = -2.26\times10^{-4}\ \mathrm{rad} \end{cases}$$

In XZ plane:

$$\begin{cases} f_4{}^{(5)} = f_{F_{t4}\to 4} = 0.0054\ \mathrm{mm} \\ f_5{}^{(5)} = f_{F_{t4}\to 5} = 0.0051\ \mathrm{mm} \\ \varphi_A{}^{(5)} = \varphi_{F_{t4}\to A} = 1.60\times10^{-4}\ \mathrm{rad} \\ \varphi_B{}^{(5)} = \varphi_{F_{t4}\to B} = 2.06\times10^{-4}\ \mathrm{rad} \end{cases} \qquad \begin{cases} f_4{}^{(6)} = f_{F_{t5}\to 4} = 0.0173\ \mathrm{mm} \\ f_5{}^{(6)} = f_{F_{t5}\to 5} = 0.0211\ \mathrm{mm} \\ \varphi_A{}^{(6)} = \varphi_{F_{t5}\to A} = 7.21\times10^{-4}\ \mathrm{rad} \\ \varphi_B{}^{(6)} = \varphi_{F_{t5}\to B} = 5.99\times10^{-4}\ \mathrm{rad} \end{cases}$$

$$\Rightarrow \begin{cases} f_{4,XZ} = f_4{}^{(5)} + f_4{}^{(6)} = 0.0227\ \mathrm{mm} \\ f_{5,XZ} = f_5{}^{(5)} + f_5{}^{(6)} = 0.0262\ \mathrm{mm} \\ \varphi_{A,XZ} = \varphi_A{}^{(5)} + \varphi_A{}^{(6)} = 8.81\times10^{-4}\ \mathrm{rad} \\ \varphi_{B,XZ} = \varphi_B{}^{(5)} + \varphi_B{}^{(6)} = 8.05\times10^{-4}\ \mathrm{rad} \end{cases}$$

Thus we have

$$\begin{cases} f_4 = \sqrt{f_{4,XY}{}^2 + f_{4,XZ}{}^2} \approx 0.0230\ \mathrm{mm} \\ f_5 = \sqrt{f_{5,XY}{}^2 + f_{5,XZ}{}^2} \approx 0.0267\ \mathrm{mm} \\ \varphi_A = \sqrt{\varphi_{A,XY}{}^2 + \varphi_{A,XZ}{}^2} \approx 8.91\times10^{-4}\ \mathrm{rad} \\ \varphi_B = \sqrt{\varphi_{B,XY}{}^2 + \varphi_{B,XZ}{}^2} \approx 8.36\times10^{-4}\ \mathrm{rad} \end{cases}$$

So the condition is verified, that

$$\begin{cases} \max(f_4, f_5) < \dfrac{L}{3000} = 0.0347\ \mathrm{mm} \\ \max(\varphi_A, \varphi_B) < 1\times10^{-3}\ \mathrm{rad} \end{cases}$$

which means that the deformation is within the safe region.

1.5.5 Critical flexional speed

$$K = \frac{3EJL}{a^2 b^2}$$

$$\Rightarrow \begin{cases} K_4 \cong 6.09 \\ m_4 \cong 1.57 \end{cases} \begin{cases} K_4 \cong 6.09 \\ m_4 \cong 1.57 \end{cases}$$

$$\omega_{cr} = \sqrt{\frac{K}{m}}$$

$$\Rightarrow \begin{cases} \omega_{cr,4} \cong 6188.85 \text{ rad/s} \\ \omega_{cr,5} \cong 898.209 \text{ rad/s} \end{cases}$$

$$\frac{1}{{\omega_{cr,tot}}^2} = \sum \frac{1}{{\omega_{cr,i}}^2}$$

$$\Rightarrow \omega_{cr,tot} = \left(\sum \frac{1}{{\omega_{cr,i}}^2}\right)^{-\frac{1}{2}} \cong 889 \text{ rad/s}$$

1.5.6 Critical torsional speed

For a disc, the moment of inertia of mass is

$$I = \frac{1}{2} m r^2 = \frac{1}{32} \rho d^4 b$$

Simplifying the gears to discs, we get

$$\begin{cases} I_4 \cong 2270 \text{ kg} \cdot \text{mm} \\ I_5 \cong 534 \text{ kg} \cdot \text{mm} \end{cases}$$

With J_p being the polar moment of inertia of the shaft section,

$$\omega_{cr,tot} = \sqrt{\frac{I_4 + I_5}{I_4 I_5} \frac{G J_p}{l}} \cong 1930 \text{ rad/s}$$

1.6. *Design or Choices for Other Components*

1.6.1 Bearings

From the given table of SKF bearing products, knowing the internal diameter $d = 22$ mm, we can easily choose the model 320/22X.
Then we need to verify the choice under the given working condition:

a. Lubricant: ISO VG 220 (viscosity 220 mm^2/s at 40°C)
b. Operating temperature: 60°C
c. Contamination level of the bearing: $\eta_c = 0.6$
d. Reliability required: 95%

For bearing No.4 which serves as a hinge-type constraint, we have

$$\begin{cases} F_{r,B4} = \sqrt{{R_2}^2 + {R_4}^2} = 1487.91 \text{ N} \\ F_{a,B4} = R_B = 433.06 \text{ N} \end{cases}$$

So, comparing with the factor given in the table,

$$\frac{F_{a,B4}}{F_{r,B4}} \approx 0.29 < e = 0.4$$

$$P_{B4} = F_{r,B4} = 1487.91 \text{ N}$$

Taking into account the type of the bearing,

$$\Rightarrow \begin{cases} L_{10} = \left(\frac{C}{P_{B4}}\right)^p = \left(\frac{11.5}{1.49}\right)^{\frac{10}{3}} \approx 909 \text{ million cycles} \\ L_{10,h} = L_{10}\frac{10^6}{60 \cdot n} = 909 \times \frac{10^6}{60 \times 120.576} \approx 1.255 \times 10^5 \text{ h} \end{cases}$$

To calculate the life expectancy at a reliability of 95%, we have to find some other factors through the tables given in 《Es08 - Cuscinetti A Rulli Conici》 (Page 3&5):

$$(100 - k)\% = 95\% \Rightarrow a_1 = 0.62$$

$$v_1 = 140 \ {}^{\text{mm}^2}/_{\text{s}} \Leftarrow \begin{cases} d_m = {}^{(d + D)}/_2 = 33 \text{ mm} \\ n = \frac{n_{in}}{u_{1-2}u_{3-4}} = \frac{1205.76}{2 \times 5} = 120.576 \text{ rpm} \end{cases}$$

$$v = 80 \ {}^{\text{mm}^2}/_{\text{s}} \Leftarrow \begin{cases} T = 60 \ ℃ \\ \text{ISO VG 220} \end{cases}$$

$$\Rightarrow \kappa = \frac{v}{v_1} = 0.57$$

$$\eta_c \frac{P_u}{P_{B4}} = 0.6 \times \frac{2.85}{1.49} = 1.148$$

thus according to the 《Es08 - Cuscinetti A Rulli Conici》 (Page 4),

$$a_{23} = 0.75$$

$$\Rightarrow \begin{cases} L_5 = a_1 a_{23} L_{10} \approx 422 \text{ million cycles} \\ L_{5,h} = a_1 a_{23} L_{10,h} \approx 5.84 \times 10^4 \text{ h} \end{cases}$$

As is required, the chosen bearing should be able to work for $[20000, 30000]$ hours. Clearly the bearing No.4 meets the need.

For bearing No.5, the same model of bearing is chosen, while it serves as a cart-type constraint instead. So similarly, we have

$$P_{B5} = F_{r,B5} = \sqrt{{R_1}^2 + {R_3}^2} = 1898.71 \text{ N}$$

$$a_1 = 0.62$$

$$a_{23} = 0.65 \Leftarrow \begin{cases} \kappa = 0.57 \\ \eta_c \frac{P_u}{P_{B5}} = 0.6 \times \frac{2.85}{1.9} = 0.9 \end{cases}$$

$$\begin{cases} L_{10} = \left(\frac{C}{P_{B5}}\right)^p = \left(\frac{11.5}{1.9}\right)^{\frac{10}{3}} \approx 404 \text{ million cycles} \\ L_{10,h} = L_{10}\frac{10^6}{60 \cdot n} = 404 \times \frac{10^6}{60 \times 120.576} \approx 5.58 \times 10^4 \text{ h} \end{cases}$$

$$\Rightarrow \begin{cases} L_5 = a_1 a_{23} L_{10} \approx 422 \text{ million cycles} \\ L_{5,h} = a_1 a_{23} L_{10,h} \approx 2.25 \times 10^4 \text{ h} \end{cases}$$

We can see that the bearing No.5 still meets the required life expectancy of $[20000, 30000]$ hours.
As a result, the chosen bearings in both positions are verified.

1.6.2 Keys

As is indicated, the choice and design of the key and the corresponding keyways are based on standard UNI 6604-69.
According to the given table, the model 'B 8x7x18 UNI 6604-69' is chosen. Following is the verification of the key.

A. Local pressure on the lateral sides

To calculate respectively the local pressure on the lateral sides of hub (gear wheel), shaft and the key, we apply the following formula:

$$p = \frac{M_t}{z \cdot \frac{d}{2}} \cdot \frac{1}{L(h - t_i)} \cdot k_{\varphi B}$$

$$\Rightarrow \begin{cases} p_{hub} = p_{key-hub} = \dfrac{39590}{1 \cdot \frac{22}{2}} \cdot \dfrac{1}{18(7-3.3)} \cdot 1.5 = 81.1 \text{ MPa} \\ p_{shaft} = p_{key-shaft} = \dfrac{39590}{1 \cdot \frac{22}{2}} \cdot \dfrac{1}{25(7-4)} \cdot 1.5 = 100.0 \text{ MPa} \end{cases}$$

To calculate the limit pressure which is correlated to material properties, we use the following formula:

$$p_{lim} = f_S \cdot R_{sn}$$

As is given, $R_{sn,hub} = 590$ MPa; $R_{sn,shaft} = 735$ MPa; $R_{sn,key} = 565$ MPa , and the collaboration factor f_S is chosen from a given table.

$$\Rightarrow \begin{cases} p_{lim,hub} = 1.5 \times 590 = 885 \text{ MPa} \\ p_{lim,shaft} = 1.2 \times 735 = 882 \text{ MPa} \\ p_{lim,key} = 1 \times 565 = 565 \text{ MPa} \end{cases}$$

For ductile material,

$$S_{F,min} \in [1.0, 1.3]$$

$$\Rightarrow \begin{cases} S_{F,hub} = \dfrac{p_{lim,hub}}{p_{hub}} = 10.9 > S_{F,min} \\ S_{F,shaft} = \dfrac{p_{lim,shaft}}{p_{shaft}} = 7.35 > S_{F,min} \\ S_{F,key} = \min\left(S_{F,key-hub}, S_{F,key-shaft}\right) = 5.65 > S_{F,min} \end{cases}$$

Clearly these three results all meet the requirement.

B. Maximum local pressure (when $\mathrm{C_{max}} = 1.6\mathrm{C_{nom}}$) on the lateral sides

$$\begin{cases} p_{hub,max} = p_{key-hub,max} = 1.6 \times p_{hub} = 129.76 \text{ MPa} \\ p_{shaft,max} = p_{key-shaft,max} = 1.6 \times p_{shaft} = 160 \text{ MPa} \end{cases}$$

In this case the maximum torque should be considered as a fatigue, as it apparently does not occur as always. As a result, the calculation of maximum limit pressure of the materials should be adjusted as:

$$p_{max,lim} = f_L(N) \cdot R_{sn}$$

As is indicated, during the life expectancy the machine will suffer the start-up condition for a maximum 1000 times, i.e.

$$N_L = 1000$$

then according to the diagram shown in《Es09 - Collegamento Albero - Ruota Dentata》(Page 9), we get

$$f_L(N) = 1.5$$

$$\Rightarrow \begin{cases} p_{max,lim,hub} = 1.5 \times 590 = 885 \text{ MPa} \\ p_{max,lim,shaft} = 1.5 \times 735 = 1103 \text{ MPa} \\ p_{max,lim,key} = 1.5 \times 565 = 848 \text{ MPa} \end{cases}$$

And in this case,

$$S_{F,min} \in [1.0, 1.3]$$

$$\Rightarrow \begin{cases} S_{F,hub} = \dfrac{p_{max,lim,hub}}{p_{max,hub}} = 6.82 > S_{F,min} \\ S_{F,shaft} = \dfrac{p_{max,lim,shaft}}{p_{max,shaft}} = 6.89 > S_{F,min} \\ S_{F,key} = \min\left(S_{F,key-hub,max}, S_{F,key-shaft,max}\right) = 5.3 > S_{F,min} \end{cases}$$

Thus the maximum local pressures are also verified.

C. Static verification of the keyway in start-up state

In this case when $C_{max} = 1.6C_{nom}$, we have

$$\begin{cases} M = M_{f,max,start-up} = 1.6 \times M_{f,max} = 1.6 \times 73.57 = 117.7 \text{ N} \cdot \text{m} \\ T = M_{t,max,start-up} = 1.6 \times M_{t,max} = 1.6 \times 39.59 = 63.3 \text{ N} \cdot \text{m} \end{cases}$$

$$\Rightarrow \frac{T}{M} = 0.538$$

In our case where both bending moment and torque are present in the shaft, we should refer to the diagram and instructions given in《Es09 - Collegamento Albero - Ruota Dentata》(Page 15) and calculate the nominal tensile stress with the following formula:

$$\sigma_{nom} = \frac{16M}{\pi d^3}\left[1 + \sqrt{1 + \left(\frac{T}{M}\right)^2}\right] \approx 120 \text{ MPa}$$

$$\Rightarrow \begin{cases} K_{tA} = 2.03 \\ K_{tsA} = 1.04 \\ K_{tB} = 2.26 \\ K_{tsB} = 1.48 \end{cases}$$

$$\sigma_{amm} = \frac{R_{sn}}{\eta} = \frac{735}{1.5} = 490 \text{ MPa}$$

$$\Rightarrow \begin{cases} \sigma_{vM,A} = \sqrt{(K_{tA} \cdot \sigma_{nom})^2 + 3 \cdot (K_{tsA} \cdot \sigma_{nom})^2} = 325.7 \text{ MPa} < \sigma_{amm} \\ \sigma_{vM,B} = \sqrt{(K_{tB} \cdot \sigma_{nom})^2 + 3 \cdot (K_{tsB} \cdot \sigma_{nom})^2} = 410.1 \text{ MPa} < \sigma_{amm} \end{cases}$$

As a result, the most critical points A and B within the keyway on the shaft are both verified under the start-up condition.

D. Fatigue verification in steady state

Suppose in both critical points A and B, the rounded radius is 1mm, thus as is calculated previously in Chapter 1.4.3,

$$q = \frac{1}{1 + {}^{\mathrm{a}}/_{r}} \approx \frac{1}{1 + {}^{0.1}/_{0.2}} = 0.67$$

$$\Rightarrow \begin{cases} K_{f,f,A} = 1 + q(K_{tA} - 1) = 1.94 \\ K_{f,f,B} = 1 + q(K_{tB} - 1) = 2.15 \end{cases}$$

Similar to the Chapter 1.4.3, we assume the bending moment to be fatigue and the torque to be static, so

$$\begin{cases} \sigma_{lim,A} = \dfrac{b_2 b_3}{K_{f,f,A}} \sigma_F = \dfrac{b_2 b_3}{K_{f,f,A}} \cdot 0.5R_m = \dfrac{0.9 \times 0.7}{1.94} \times 0.5 \times 1030 = 167.24 \text{ MPa} \\ \tau_{lim,A} = 0.58R_{sn} = 0.58 \times 735 = 426.30 \text{ MPa} \end{cases}$$

$$\Rightarrow H_A = \frac{\sigma_{lim,A}}{\tau_{lim,A}} = 0.39$$

$$\begin{cases} \sigma_{lim,B} = \dfrac{b_2 b_3}{K_{f,f,B}} \sigma_F = \dfrac{b_2 b_3}{K_{f,f,B}} \cdot 0.5R_m = \dfrac{0.9 \times 0.7}{2.15} \times 0.5 \times 1030 = 150.91 \text{ MPa} \\ \tau_{lim,B} = 0.58R_{sn} = 0.58 \times 735 = 426.30 \text{ MPa} \end{cases}$$

$$\Rightarrow H_B = \frac{\sigma_{lim,B}}{\tau_{lim,B}} = 0.35$$

and also, by taking into account only the alternative component of tensile stress, which is the bending moment, and supposing the alternative component of shear stress to be its medium, we get:

$$\begin{cases} \sigma_{a,A} = \sigma_{a,B} = \dfrac{32M_{f,max}}{\pi d^3} = 70.38 \text{ MPa} \\ \tau_{a,A} = \tau_{a,B} = \tau_m = \dfrac{16M_t}{\pi d^3} = 18.94 \text{ MPa} \end{cases}$$

$$\sigma_{amm} = \frac{\sigma_{lim}}{\eta} = \frac{215.85}{1.5} = 143.9 \text{ MPa}$$

$$\Rightarrow \begin{cases} \sigma^*_{GP,A} = \sqrt{{\sigma_{a,A}}^2 + {H_A}^2 {\tau_{a,A}}^2} = 70.77 \text{ MPa} < \sigma_{amm} \\ \sigma^*_{GP,B} = \sqrt{{\sigma_{a,B}}^2 + {H_B}^2 {\tau_{a,B}}^2} = 70.69 \text{ MPa} < \sigma_{amm} \end{cases}$$

which means the fatigue condition in critical points A and B is verified, thus the overall design of the key and its keyways is verified.

1.7. *Summary of the Overall Design Characteristics*

Gear Pair No. 3&4:

$$\begin{cases} m_n = 1.21 \\ m_t = 1.3021 \end{cases} \quad \begin{cases} z_3 = 16 \\ z_4 = 80 \end{cases}$$

$$\begin{cases} d_{p3} = 20.83 \text{ mm} \\ d_{p4} = 104.17 \text{ mm} \end{cases} \Rightarrow u_{3-4} = 5.001$$

Considering the overall machine size and taking into account the safety margin, it is then decided a gear thickness

$$b_4 = 18\text{mm}$$

Gear Pair No. 5&6:

$$\begin{cases} m_n = 1.751 \\ m_t = 2.0646 \end{cases} \quad \begin{cases} z_5 = 15 \\ z_6 = 62 \end{cases}$$

$$\begin{cases} d_{p5} = 30.97 \text{ mm} \\ d_{p6} = 128.03 \text{ mm} \end{cases} \Rightarrow u_{3-4} = 4.133$$

Similarly, it is then decided

$$b_5 = 25\text{mm}$$

The whole length of the shaft is $L = 104\text{mm}$, and the fundamental diameter is defined as $d = 22\text{mm}$. Taking into account the thickness of the bearing (15mm) and the symmetry of the structure, the shoulders are designed (referring to the Section 2.1.1.1)

The key is chosen as type B 8x7x18 UNI 6604-69, and the dimension of keyway also refers to Section 2.1.1.1.

2. FE MODEL FOR NUMERICAL CALCULATION

The FE analysis of the central shaft is carried out in the software 'Abaqus', under 'general, static' condition, and with 'linear-direct' approach. After the 3D model with previously designed geometry is built in CREO 3.0, it is imported into Abaqus, in order to assign mesh partition, loads, constrains and conduct the final FE calculation. In addition, a segmentation of the central shaft is made, in order to make it much easier to simulate the working conditions in different phase angle during rotating.

2.1. *Geometry and mesh of the parts*

There are two parts in the analysis, for the reason previously elaborated.

2.1.1 Description of Component 1

The Component 1 represents the core (main) part of the central shaft, i.e. the shaft without Gear 5.

2.1.1.1 Geometry

The geometry of Component 1 has already been described in Section 1.7. As is shown in Fig 14, the Component 1 has a basic diameter 22 mm and a thicker cylinder with diameter 27 mm, according to the standard provided by SKF. In addition, a keyway beside the thicker cylinder, which transmits power from Gear 4 to the central shaft, is presented in the model, in accordance with the previous design

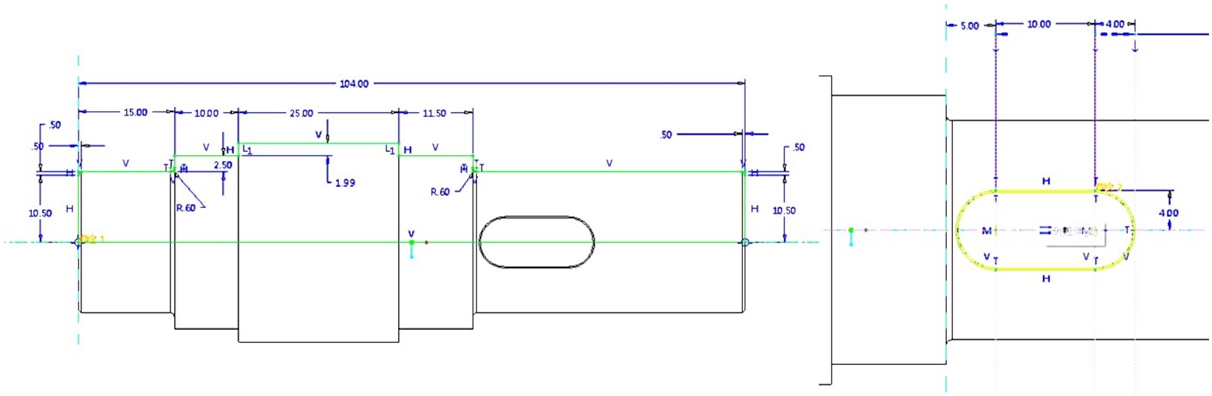

Fig 14: GEOMETRY OF THE COMPONENTS

2.1.1.2 Mesh

Basing on the geometry of the existing part and its irregular property, an element type of '10-node quadratic tetrahedron' and the "free" mesh method with tetrahedron are applied to obtain the result shown in Fig 15.

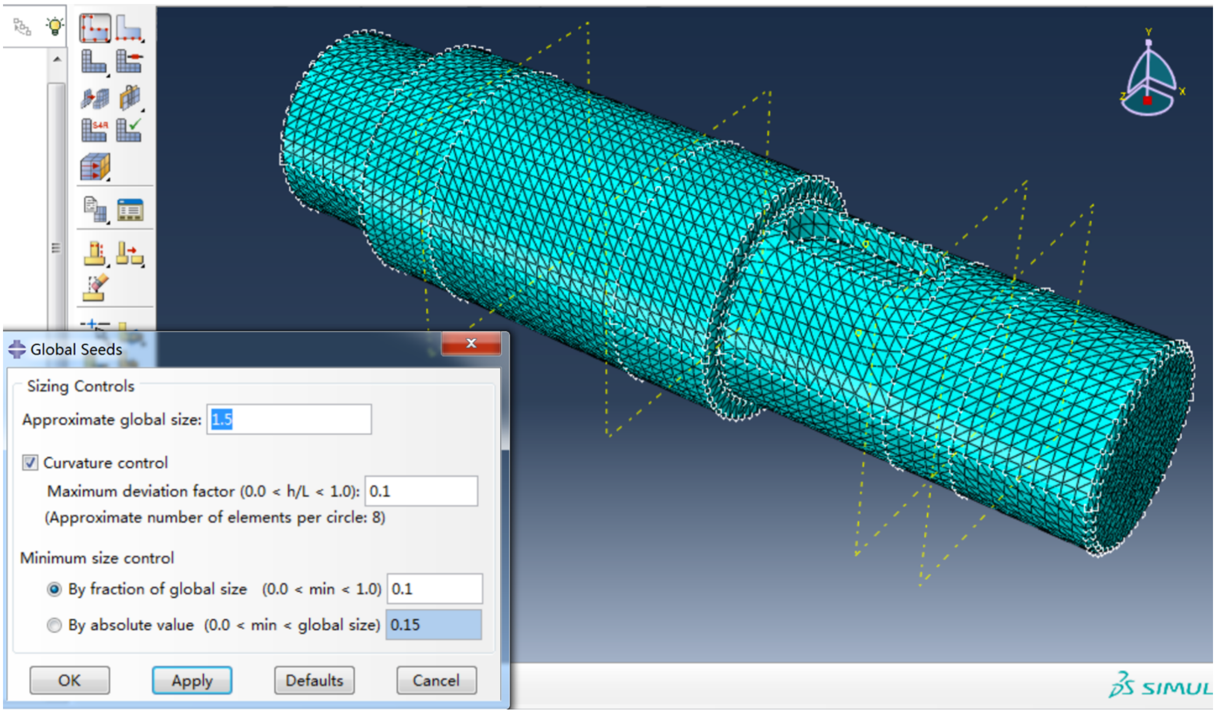

Fig 15: RESULT OF COMPONENT 1 MESHING

2.1.2 Description of Component 2

The component 2 with a column geometry represents the Gear 5 through which the power is transmitted from the central shaft to the output shaft. This component is designed to make it easier to analysis the central shaft in different phase angles.

2.1.2.1 Geometry

According to the design of the gear, the length of the component 2 is 25 mm, and the outer diameter is equal to the pitch diameter of Gear 5, i.e. 30.97 mm. The inner diameter here is made identical with the thicker cylinder diameter in Component 1, i.e. 27 mm.

2.1.2.2 Mesh

Considering the fact that the geometry of the column is very regular, the "sweep" method is applied for the mesh and the element type is again chosen as "an 8-node linear hex". In the area that represents the teeth in contact, a more intensive mesh control is applied. The result is given in Fig 16.

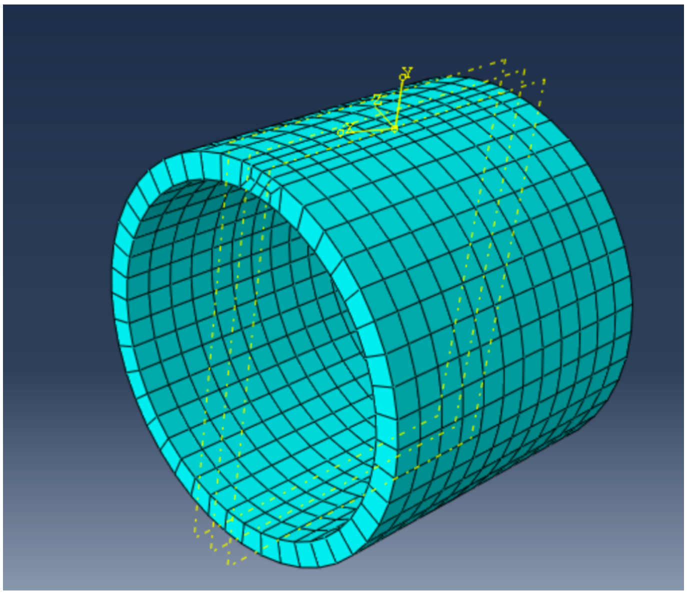

Fig 16: RESULT OF COMPONENT 2 MESHING

2.2. ***Material***

The material of the interested part is assumed to be perfectly elastic, with the elastic modulus is $E = 210$ GPa, Poisson's ratio $\nu = 0.33$, and the density $\rho = 7850\ \mathrm{kg/m^3}$.

2.3. ***Interactions***

There are in total 5 interactions applied to the model, as are showed in Fig 17. In detail, four 'Coupling' are applied simulating respectively the effect of the two bearings, the Gear 4 and the active tooth on Gear 5; and one 'Tie' is applied representing the interaction between the Component 1&2, since they are essentially one complete piece.

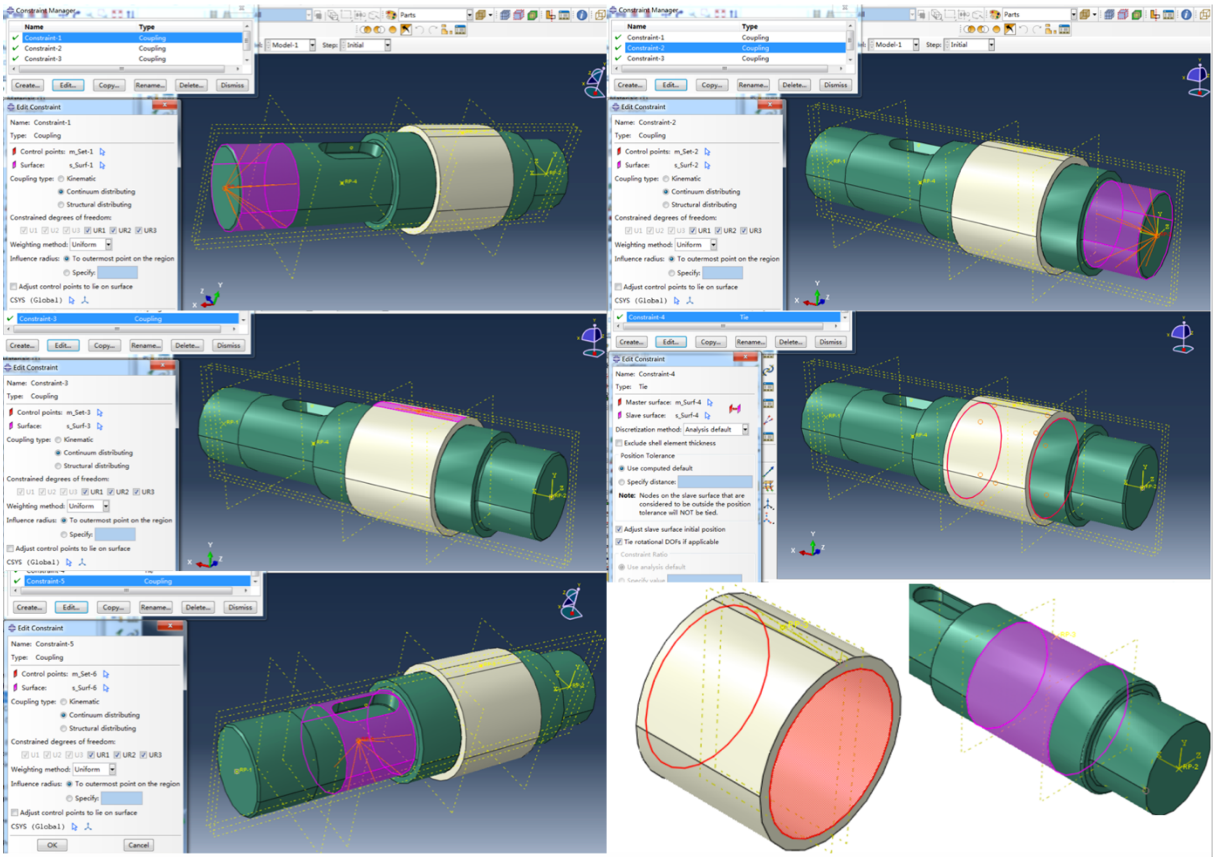

Fig 17: ILLUSTRATION OF THE INTERACTIONS

2.4. ***Constrains and Loads***

2.4.1 Constrains

There are in total 3 constrains: two respectively in the center point of the two bearing, with the one closer to Gear 5 acting as cart and the one closer to Gear 4 acting as hinge; and the other one in at the tooth of Gear 5, to simulate the situation in the instant that the power is transmitted from Gear 5 to Gear 6, which requires a new local reference system for the reason that the gear is helical. The different settings of the constrains are shown in Fig 18.

It is to be highlighted that here it is defined a different order of hinge and cart as it was in Section 1.4.3, for the reason that in the software the external force is effective only if it is applied at a cart constraint. It should make no difference to the final result.

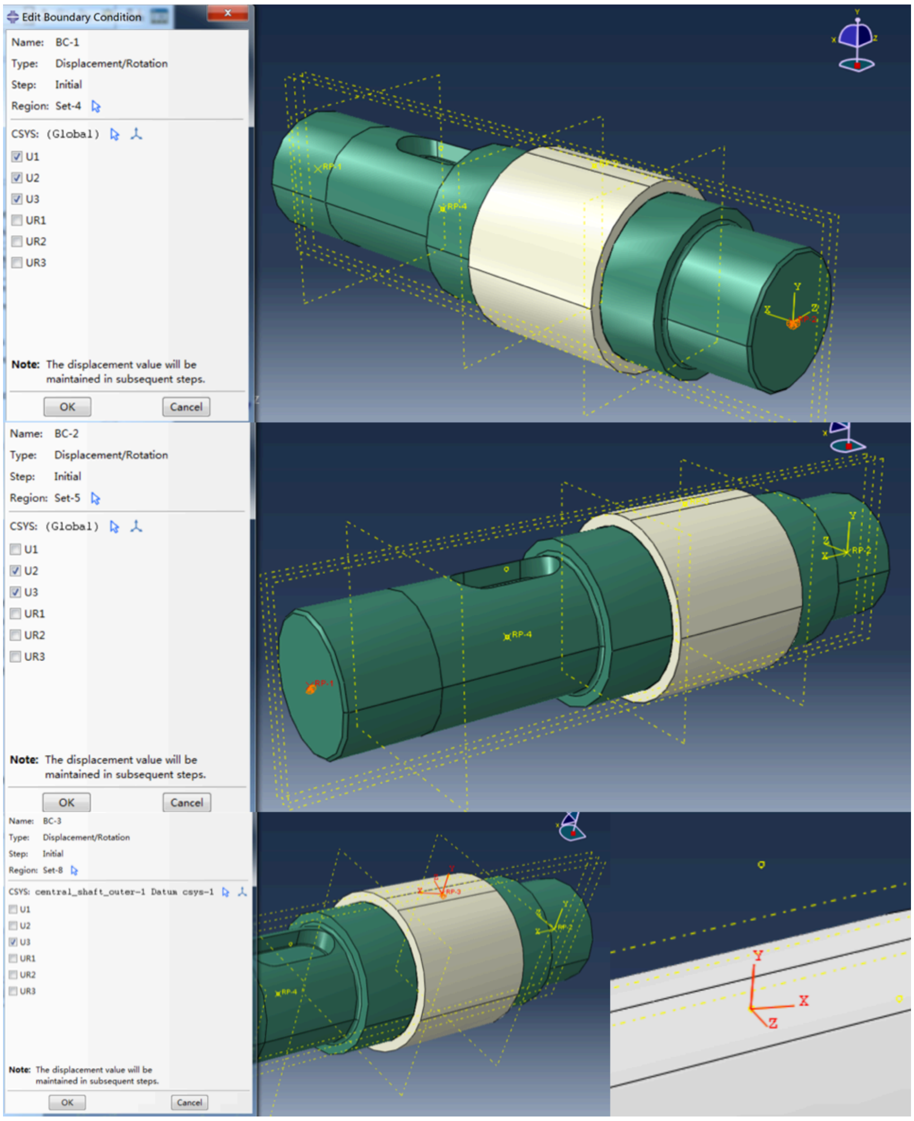

Fig 18: ILLUSTRATION OF THE CONSTRAINTS

2.4.2 Loads

In order to simulate the true working condition, there are three loads applied, all generated by the Gear 4 which transfers the power into the central shaft through the key and the keyway. Thus, the details of the loads are as given in the Fig 19.

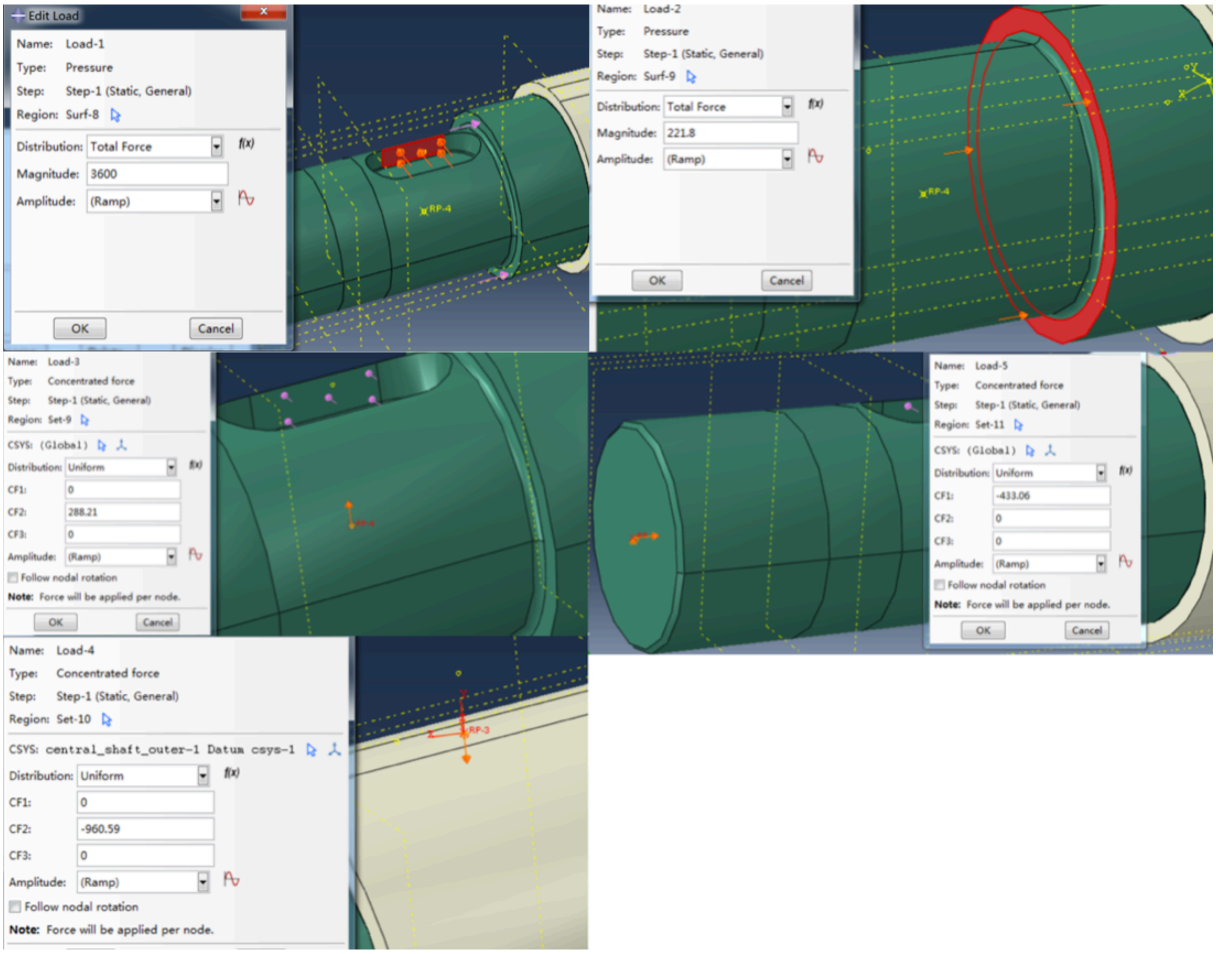

Fig 19: ILLUSTRATION OF THE LOADS

3. NUMERIC RESULTS AND THE COMPARISON WITH THE ANALYTICAL RUSELTS

3.1. *Simulation Results*

The overall Von-Mises Stress state is given in Fig 20.

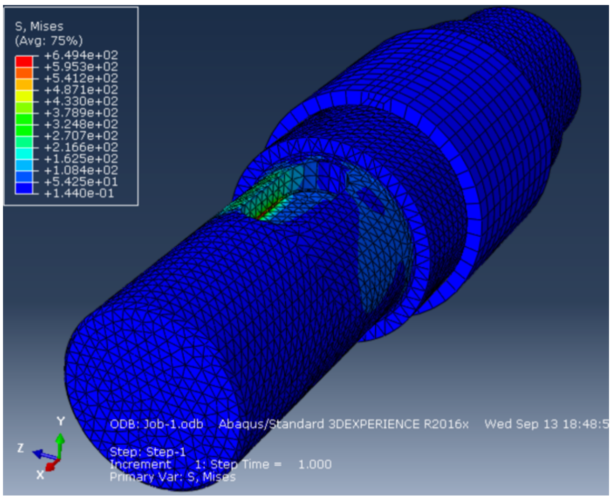

Fig 20: THE OVERALL VON-MISES STRESS STATE

3.1.1 State of Component 1

The Von-Mises Stress state of the Component 1 is given in Fig 21.

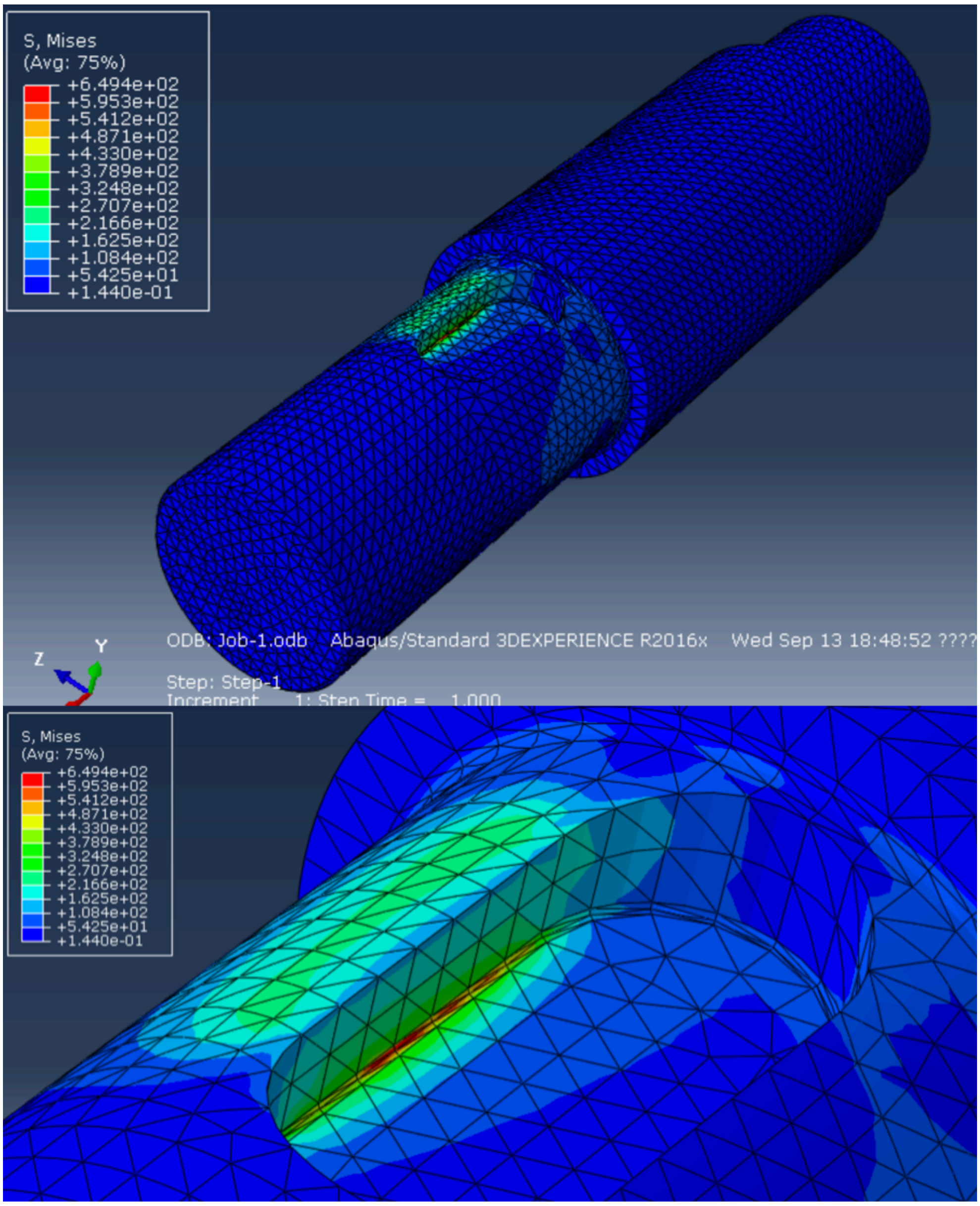

Fig 21: THE VON-MISES STRESS STATE OF COMPONENT 1

After creating a path shown in Fig 22, we can measure the deflexion both in XY plane and XZ plane, and the result is shown in Fig 23. The overall deformation status is given in Fig 24. From every aspect the deformation on the piece is always less than $\frac{L}{3000} = 0.0347\ \text{mm}$, which indicates that the shaft designed meets the requirement. The FEM result is also identical with the analytical result.

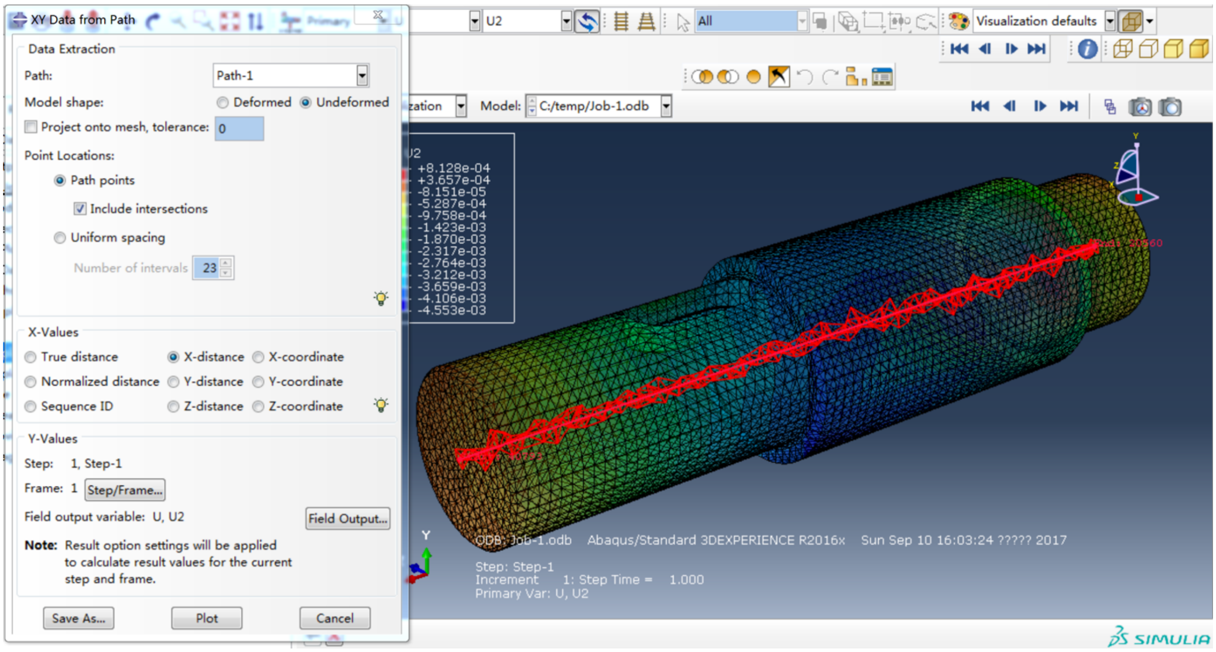

Fig 22: ILLUSTRATION OF THE PATH CREATED

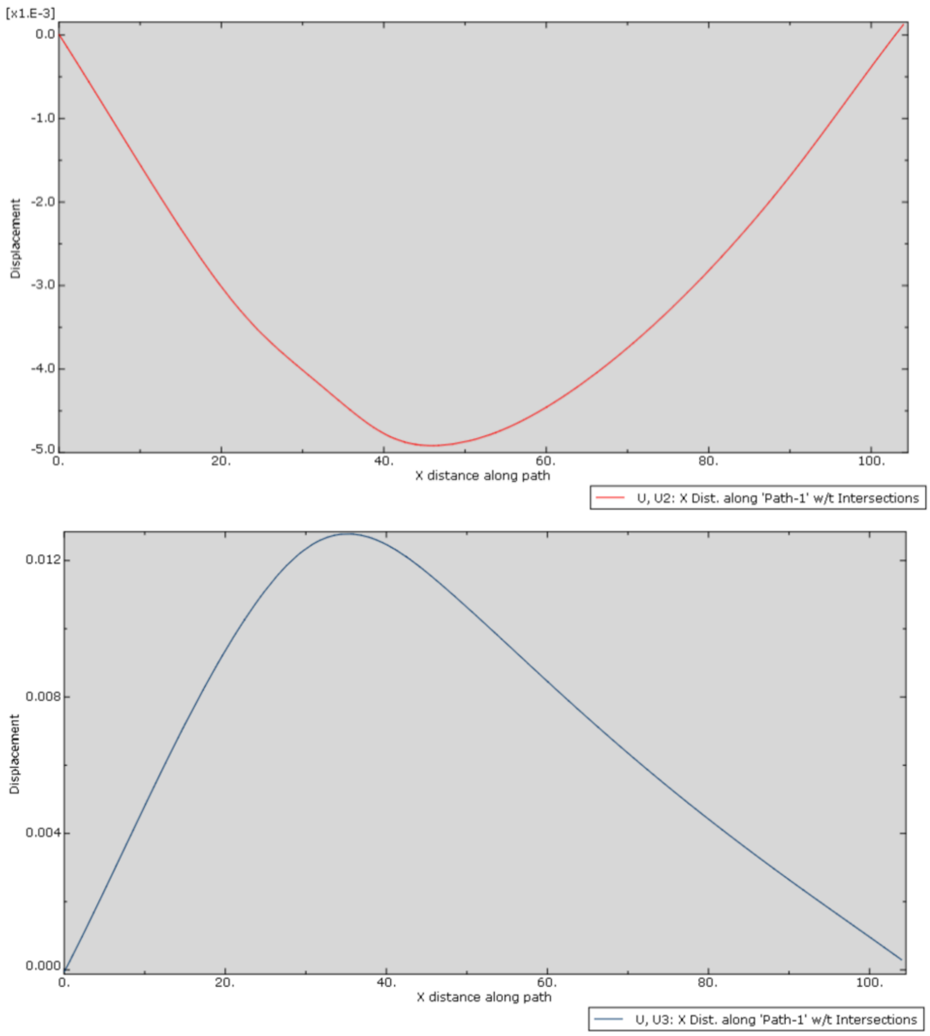

Fig 23: PLOT OF THE DEFLEXION IN XY & XZ PLANES

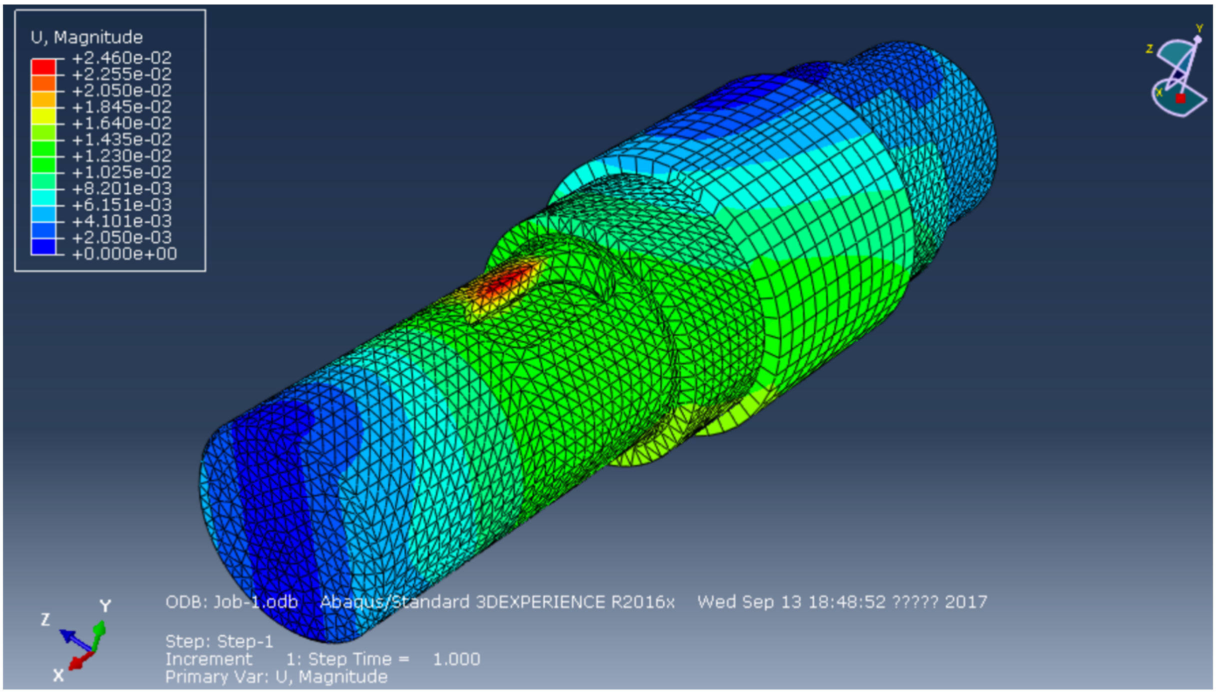

Fig 24: THE OVERALL DEFORMATION OF THE COMPONENT 1

3.1.2 State of Component 2

The Von-Mises Stress state of the Component 1 is given in Fig 25, and the overall deformation status is given in Fig 26.

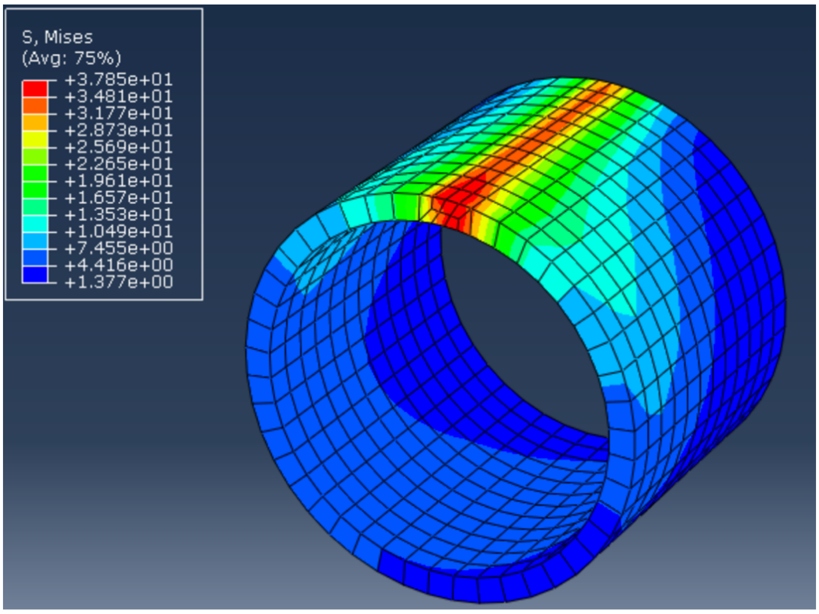

Fig 25: THE VON-MISES STRESS STATE OF COMPONENT 2

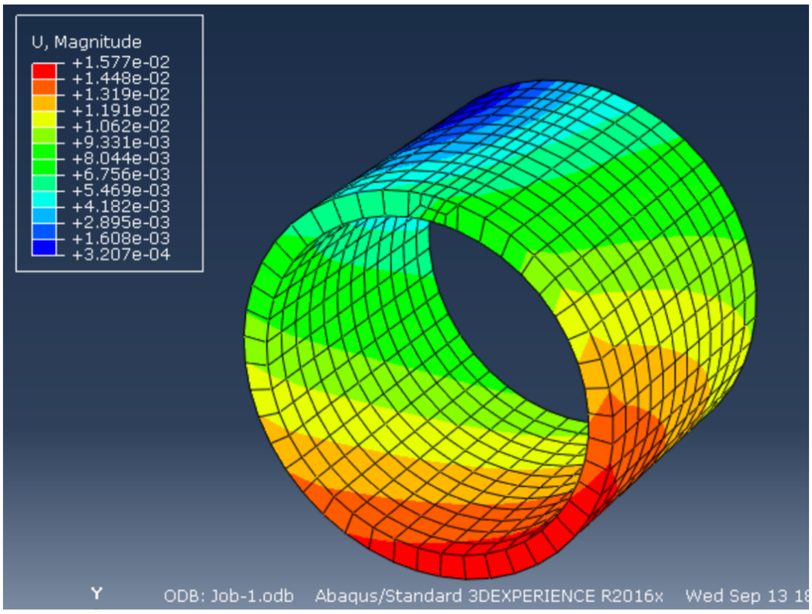

Fig 26: THE OVERALL DEFORMATION OF THE COMPONENT 2

3.2. ***Verification of the results***

3.2.1 Comparisons of analytical/numerical constrain forces

To comparing the two groups of results, the analyses should be done under the same working condition, as a result the working piece in the software is rotated an angle equaling to 180°.

The numerical result of the reaction forces is shown in the Fig. 27. As was calculated in Section 1.4.3, the analytical result is

$$\begin{cases} R_1 = 315.58\text{ N} \\ R_2 = 356.80\text{ N} \end{cases}$$
$$\begin{cases} R_3 = -1872.30\text{ N} \\ R_4 = -1444.50\text{ N} \end{cases}$$

whereas the analytical result is

$$\begin{cases} R_1 = 666.975\text{ N} \\ R_2 = 581.825\text{ N} \end{cases}$$
$$\begin{cases} R_3 = -3562.27\text{ N} \\ R_4 = -2690.42\text{ N} \end{cases}$$

It turns out that the two groups of results are quite different, and it is considered inevitable in our case.

The main reason leading to the difference is the load (pressure) applied on the keyway in ABAQUS. This load was supposed to simulate the key-connection that conducts the force from Gear No.3 to Gear No.4 and thus to the shaft interested. In analytical analysis, this motoring force equals to $F_{t4} = \frac{2C}{d_{p4}} = 760.14$ N, and it is further decomposed into a radical force in XZ plane equaling to 760.14 N and a torque. Meanwhile in the FE analysis, in order to obtain a torque that is essential in the whole project, the force applied on keyway lateral side is defined as approximately 4000 N, which results in a much larger radical force in XZ plane, and then cause a difference in reaction forces in the constraints.

The second reason is the axial force generated through transmission F_{a4} should in reality lead to a bending moment M_{a4} as is calculated during analytical analysis, whereas in FE analysis it is ignored. But this error is acceptable due to the fact that the magnitude of M_{a4} is relatively small.

On the whole, with the motoring torque set to be correct, and the loads set to be larger than in real working condition, the FE analysis still gives an outcome stating that the shaft would not fail, the overall result should be considered valid.

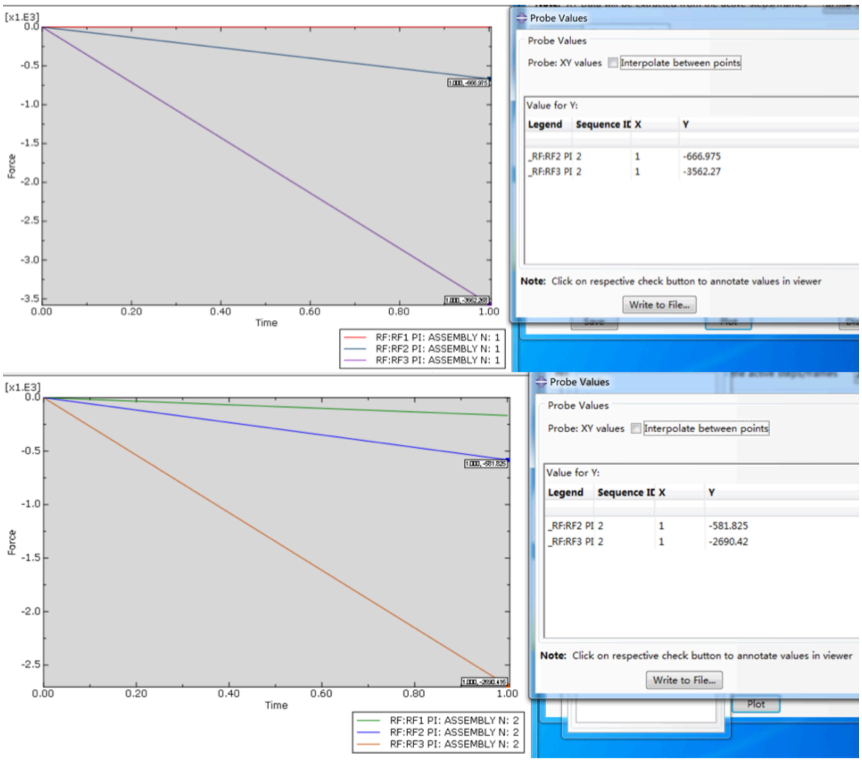

Fig 27: THE NUMERICAL RESULT OF THE REACTION FORCES

3.2.2 *Verification of analytical/numerical results of K_t*

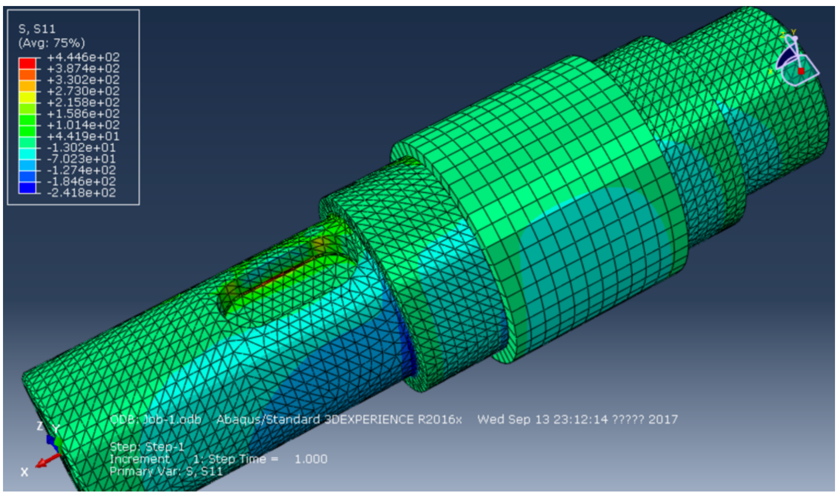

Fig 28: THE NUMERICAL RESULT OF THE NORMAL STRESS

From the Section 1.6.3 we have $\sigma_{nom} = \frac{16M}{\pi d^3}\left[1 + \sqrt{1 + \left(\frac{T}{M}\right)^2}\right] \approx 120$ MPa and in the most critical area Point B, we have $K_{t,ANA} = 2.26$.
From the above Fig 28 we can find that the maximum normal stress is equal to $\sigma_{max,FEM} =$ 444.6 MPa, thus we get

$$K_{t,FEM} = \frac{\sigma_{max,FEM}}{\sigma_{nom}} = \frac{444.6}{120} = 3.705$$

Similar with the circumstance in the previous section, the difference in the two results is due to the error in simulating the force conducted though the keyway, which causes the change of the maximum bending moment M, thus the change of the σ_{nom}.

3.3. *General consideration*

Generally speaking, every moment of rotation should be taken into account. As a result multiple analyses were carried out in ABAQUS by applying ‘instant rotation’ in ‘Assembly’ modulus. The results are given in Fig 29&30.

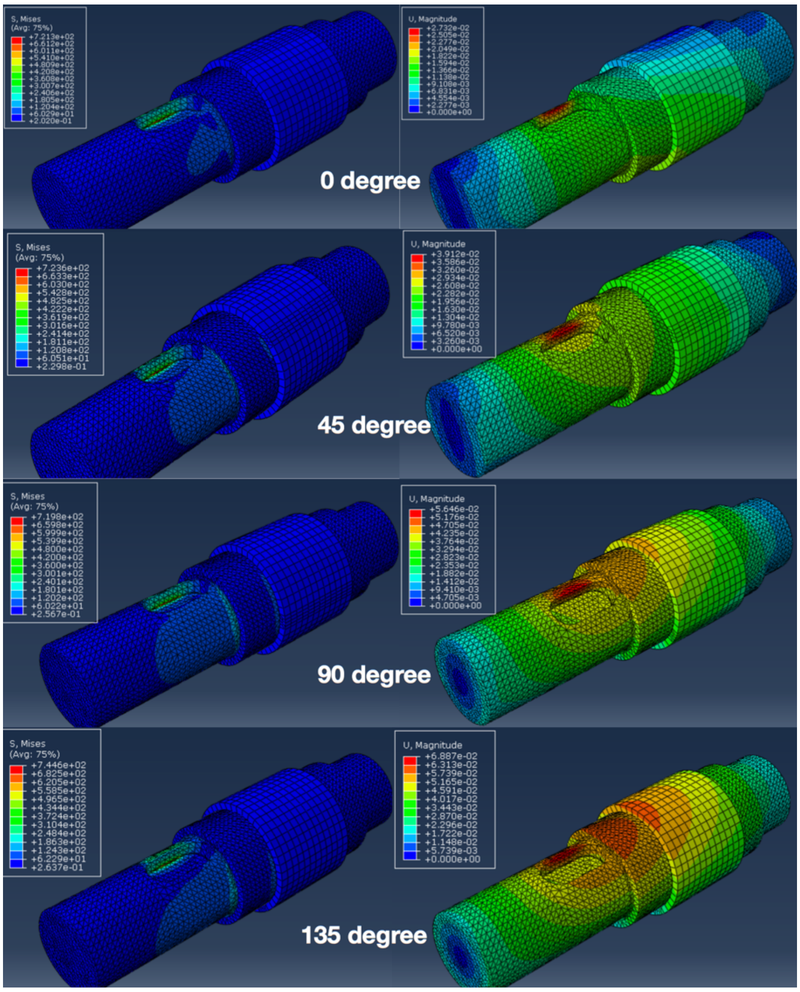

Fig 29: MULTIPLE ANALYSES FOR DIFFERENT ROTATION ANGLES (PART 1)

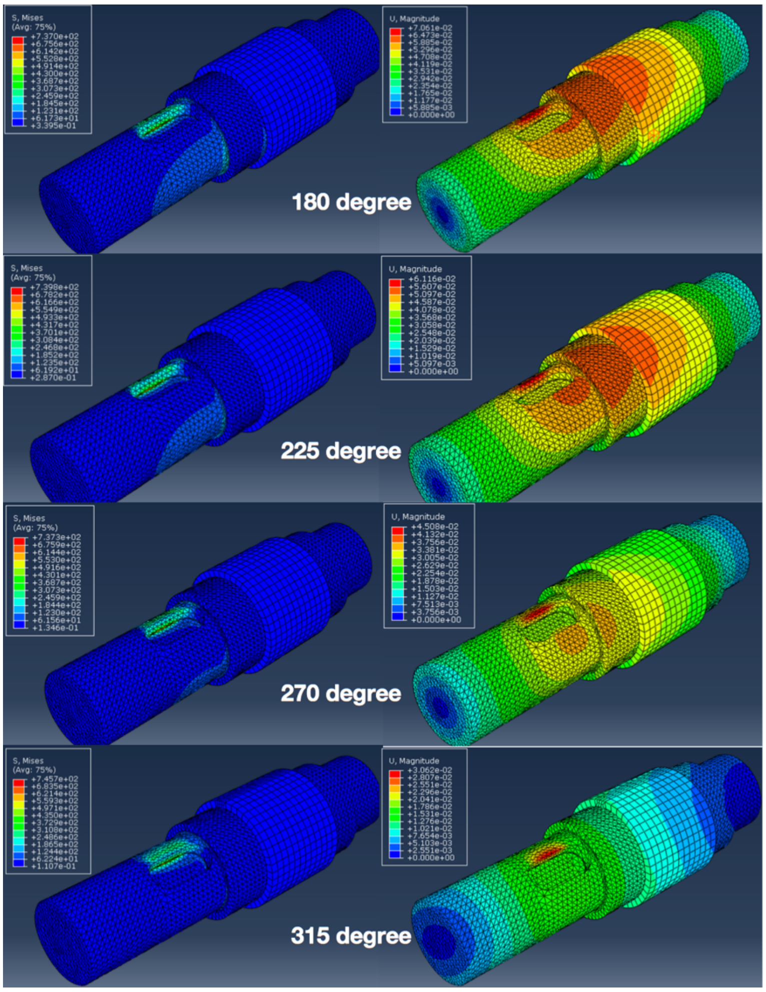

Fig 30: MULTIPLE ANALYSES FOR DIFFERENT ROTATION ANGLES (PART 1)

From these analyses we found that the most critical angle should be between 135 and 180 degrees. To determine a precise critical angle, more analyses should be executed, that would take much time, for which reason within this project no more discussion is made.

The FEM method, including the set of loads and constraints in this project is to a large extent instructed during the lab course. However, in this case, the fact turns out that there exist some errors that are inevitable, as was specified in the previous section. And the reason why the result is still valid is also claimed in Section 3.2.1.

Thus in short words, the FEM result may not precisely simulate the reality, while it does verify that the work piece interested (the central shaft) meets all the requirements and will not fail the normal working condition. And for sure the final determination of the shaft design should still refer to the cooperation of other components in the machine.

4. Drawings

See attachments.

5. CONCLUSION

In this project, a central shaft is designed, including dimensioning and verification both through analytical and numerical methods, and the two groups of results are compared in order to demonstrate the credibility of the overall analysis.

As for the weaknesses in this project, as was commented in Section 3.2.1, the main one is to represent forces transmitted through the key with a single large pressure on the lateral side of keyway. This can result in a much larger radical force on XZ plane, which eventually make unprecise the overall analysis. However, since this simulated force is much bigger than the real one and the result still shows that the workpiece satisfies all the needs, we can consider the FEM result to be valid, although not precise. Except this, all the constraints, boundary conditions and loads all simulate the real working conditions well.

This project shows that in practical engineering procedures, FE simulation is a far more complex work than imagine, because in order to make the result accordance with the reality, a lot of factors and every working condition expected should be taken into account, like the different angles during rotation and the reaction forces. As a result, this project is successful and a meaningful one as well.

Milano, 17 Sep 2017

Bibliography

[1] Es07 - Dimensionamento E Verifica Dell'Albero Centrale

[2] Lab08 - Modellazione FEM Albero Centrale - Parte 1

[3] Lab09 - Modellazione FEM Albero Centrale - Parte 2

MASSA / MASS	TEMPER	CENTRAL SHAFT	DIS. / DWG.
SCALA / SCALE 1:0.8		(A4) R CIU 80 U03A	PART.3D / PART.3D
TOLL.GEN.LAV. / FORI TOLL. + / ALBERI TOLL. –	GEN.MACH.TOL. / HOLES TOL. + / SHAFT TOL. –	MATERIALE / MATERIAL — QUALITA / QUALITY: 16MnCr5	* T.REV.3D / REV.PART.3D
		TRATT.TERM. / THERMAL TREAT.: Cmt–Tmp	CODICE / CODE
		RIVESTIMENTO / COVERING	
			DATA / DATE: 17/09/2017
			DIS. / DRAFTMAN.: CAI ZHONGTIAN — CONTR. / SUPERV.

* for u=3.13 Lmt 16MnCr5 EN 10084–98

class set of teeth 8 before the heat treatment for u=5.2

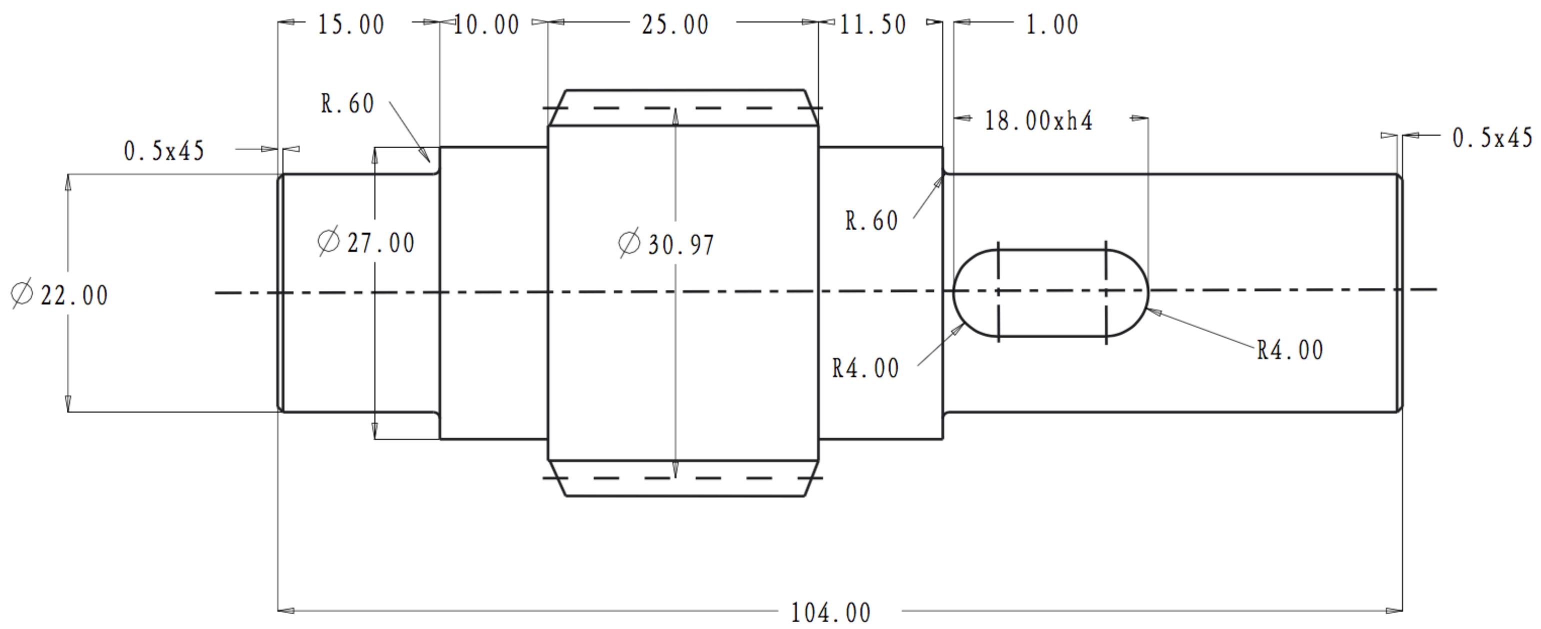

DATA / DATE	17/09/2017	MV	MR 3I 80 UP2A	DIS. / DWG.
DIS. / DRAFTMAN.	CAI ZHONGTIAN			REV.DIS. / DWG.REV.
				DATA.REV. / REV.DATE

IMPORTANTE / IMPORTANT

- il valore dopo la barra indica la quantita maggiore di 1
  Value given after the bar states quantity when it is more than 1
- Per la richiesta di pezzi di ricambio indicare sempre la relativa designazione, il tipo di riduttore, il numero di tavola e il rapporto di trasmissione
  When ordering spare parts always state their designation, gear reducer type, this drawing number and transmission ratio